Sustainable Cities and Society 101 (2024) 105122

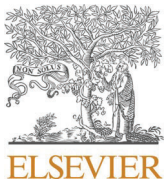

Contents lists available at ScienceDirect

Sustainable Cities and Society

journal homepage: www.elsevier.com/locate/scs

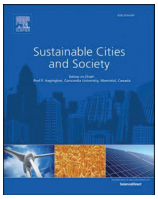

Decoding vibrant neighborhoods: Disparities between formal neighborhoods and urban villages in eye-level perceptions and physical environment

Jin Rui [a,*], Xiang Li [b]

[a] Department of Spatial Planning, Technical University Dortmund, August-Schmidt-Straße 10, Dortmund 44227, Germany
[b] School of Architecture, Urban Planning Department, The University of Hong Kong, Hong Kong

ARTICLE INFO

Keywords:
Neighborhood vitality
Eye-level perceptions
Neighborhood environment
GTWR
XGBoost

ABSTRACT

Vibrant neighborhoods play a pivotal role in the human well-being and social cohesion. However, existing research amalgamates vitality discussions of varied functions, failing to offer nuanced insights for specific neighborhood planning. Another gap emerges from the lack of research focusing on cultivating neighborhood vibrancy based on bottom-up spatial perceptions at the eye-level. Therefore, our study delves into the spatial and temporal disparities in vitality between formal neighborhoods and urban villages. Both real and virtual indicators are employed to measure the physical and digital vitality of neighborhoods. We incorporate eye-level perceptions as a new explanatory variable based on the physical environment. Our findings suggest that real vitality exhibits a modest morning and evening peak on weekends, while virtual vitality continually increases and peaks at night. In addition to enhancing green and enclosed neighborhood environments, improving public transportation options that replace reliance on motorized travel could facilitate formal neighborhood vitality. Regarding urban villages, clear rights-of-way can boost commuting efficiency, spatial accessibility and road safety, while the provision of ample public facilities and public spaces fosters the creation of "15-minute living circles." The differentiated planning recommendations could offer valuable insights to promote livable neighborhoods and ultimately help to improve human well-being.

1. Introduction

Spatial vitality refers to the capacity of a place to attract people for different types of activities (Chen et al., 2023; Row & Jacobs, 1962; Lee and Kang, 2022; Wu et al., 2023). Row and Jacobs (1962) first introduced the concept of vitality in her book *The Death and Life of Great American Cities*. She argued that vitality served as the cornerstone of livable cities and was greatly influenced by the spatial characteristics of urban environments. The concept of neighborhood vitality (NV) is important in creating livable communities that are attractive to residents. Neighborhoods with high levels of vitality are often considered desirable places to live, that improve residents' physical and mental health (Chen et al., 2023; Li et al., 2022; Rui and Othengrafen, 2023; Yue et al., 2019). Simultaneously, enhancing NV aligns with the pursuit of "good health and well-being" and "sustainable cities and communities" in Sustainable Development Goals (SDGs) (United Nations, 2017).

Recently, Jiang Haiyan (2023) proposed a new conceptualization of real and virtual vitality, that fundamentally aligns with the concepts of real and virtual vitality proposed by Wang (2019). However, Wang's notion of virtual vitality may have different meanings within the field of psychology, leading to misconceptions in the conceptualization of vitality. Therefore, this study opts for the latest terms, "real and virtual vitality," to comprehensively characterize urban vitality. Real vitality characterizes embodied vitality and includes four categories: society, economy, culture, and environment. Specifically, real vitality can be observed, such as people's activities of people in urban spaces (Oldenburg, 2001). Virtual vitality, meanwhile, refers to new forms of NV in the context of digitalization, in the field of cyberspace. The concept originates from the integration of digital network media with urban geographic elements mentioned by McQuire (2017). Digital media liberate people from "place" and become an important form of place-making. This study is based on the theory of real and virtual vitality. Furthermore, studies indicate that variations in light and mood

* Corresponding author.
E-mail address: jin.rui@tu-dortmund.de (J. Rui).

https://doi.org/10.1016/j.scs.2023.105122
Received 5 September 2023; Received in revised form 10 December 2023; Accepted 12 December 2023
Available online 17 December 2023

across different times can influence vitality changes (Ryan et al., 2010; Smolders et al., 2013),considering that urban vitality during weekdays is affected by working-oriented travel, which exhibits traffic inertia (Sevtsuk and Ratti, 2010) with regular and pronounced peak periods. Weekend travels have more diverse purposes and unpredictable results than weekday travels (Hu, Xu, Shen, Shi, & Chen, 2018b; Lai et al., 2022), making the investigation of NVduring weekends insightful.

Vitality is closely related to the built environment (Li et al., 2022; Liu and Shi, 2022; Ye et al., 2018; Yue et al., 2019; Zhang et al., 2021a). Some previous studies refer to the 3D (density, diversity, and design), and 5D (density, diversity, design, distance to transit, destination and accessibility) frameworks for variable selection (Chen et al., 2022a; Chen et al., 2022b; Li et al., 2022; Wu et al., 2022). In addition to the physical built environment, human perception of urban space affects preferences for staying and path selection, leading to spatial differentiation in vitality (Kang et al., 2021).

Although the notion and significance of vitality have garnered extensive acknowledgment and discourse, there are gaps in specific research methods and scope. Existing studies often lean toward macro-level observations, overlooking the subtle differences and dynamics at the neighborhood and resident levels. To be specific, previous studies have focused on entire cities. However, Wu et al. (2023) emphasized that urban function was the dominant variable in vitality differences. Therefore, focusing on a particular functional area will lead to more insightful results. Second, there is currently no systematic framework for characterizing NV. The varying definitions of vitality have led to misinterpretation and increased ambiguity in vitality characterization. Third, the synergistic contribution of eye-level perceptions and the physical environment to NV remains to be explored. Fourth, studies have adopted single models to analyze the causes of NV (Chen et al., 2023; Li et al., 2022; Liu and Shi, 2022; Shi et al., 2023; Zhang et al., 2021a). However, it is difficult for a single model to characterize the complex relationship between the variables and vitality. To bridge these research gaps, we propose a central research question: What factors influence the vitality of different neighborhoods, and how can we offer planning suggestions to enhance NV based on the underlying mechanisms? Building here,three sub-questions follow: How can we quantify NV based on the latest vitality theories? How do the physical neighborhood environment and eye-level perceptions relate to NV? To what extent do spatial perceptions complement physical neighborhood environments?

This study's contribution lies in two main areas: Theoretically, it redefines NV through the lens of real and virtual interactions, validating key hypotheses that emphasize the multidimensionality of vitality. By integrating empirical validation with theoretical discourse, our research challenges existing assumptions and broadens the conceptual realm oNV. Practically, our study entails targeted improvements for formal neighborhoods (FNs) and urban villages (UVs). We advocate a resident-centered, bottom-up planning approach, providing guidance for optimizing streetscapes, transportation systems, and public facilities. This approach promotes the realization of the "Shenzhen Urban Village Comprehensive Improvement Master Plan (2019-2025)" (Shenzhen Planning & Natural Resources, 2019) and the broader goal of creating livable, vibrant urban communities.

2. Literature review

2.1. The definition and measurement of spatial vitality

Urban vitality is the lifeblood of a city, reflecting not only the social liveliness, population density, and living standards within urban spaces, but also serving as a key factor in promoting healthy urban development and enhancing city competitiveness (Huang et al., 2022; Jiang Haiyan, 2023; Lee and Kang, 2022; Li et al., 2022; Xia et al., 2020). Traditionally, vitality is a concept based on physical and actual space. Row and Jacobs (1962) argued that the "life" in a city comprised pedestrian activities on urban streets, and thus urban vitality was closely tied to public life in streets, squares, and parks, contributing to unique community characteristics. This traditional "physical activity" primarily takes place within a city's physical spaces of and is typically constructed within specific social contexts (Marquet and Miralles-Guasch, 2015; Xia et al., 2020).

Recent research emphasizes the impact of digital transformation on urban vitality (Jiang Haiyan, 2023). In particular, the overall level of development of financial inclusion promotes a city's economic vitality (Sun & You, 2023). Digital technologies and new media are creating new urban spaces by altering how people produce, live, and socialize (Wang, 2019), prompting the study of urban vitality to extend into virtual spaces. For instance, a city's virtual vitality has been assessed by analyzing the spatial distribution of urban Wi-Fi (Kim, 2018) . In this digital age, physical contact is no longer the sole prerequisite for vitality; online interactive technologies are revolutionizing traditional face-to-face social activities. Consequently, there is an urgent need for empirical studies to quantify and validate the hybridity of physical and virtual vitality in urban spaces (Antoniadis & Apostol, 2014; Forlano, 2013; Kim, 2018).

The current application of big data to assess urban spatial vitality has become a new research interest. As shown in Table 1, scholars have measured vitality based on multiple data sources. Previous research utilized a solitary data source to assess vitality. For instance, the Baidu heat map has frequently been employed to delineate the spatial distribution of population density (Fan et al., 2021; Li et al., 2019; Lyu and Zhang, 2019). It can provide a highly accurate representation of the real-time population density across diverse locations and times. Weibo check-in, a form of location-based data, has also been used to measure the digital popularity and attractiveness of specific locations among app users (Huang et al., 2022). Similar data sources comprise Easygo (Wu et al., 2023), Tencent's location data (Chen et al., 2022b), and mobile-phone data (Chen et al., 2023).

Recent studies have started to leverage multivariate data for vitality assessment. Ou et al. (2021) utilized POI, land use, and Weibo check-in data. Upon data standardization, all the variables were assigned equal weights, and these were then combined to calculate a vitality value. Nonetheless, this equal-weighting method fails to consider the variable-characterization capacities of the different data types. In contrast, Shi et al. (2023) employed nighttime lighting, and Weibo check-in data, cultural POI, and NDVI, using the entropy weighting method to derive the vitality value, which appears more convincing. Liu and Shi (2022) applied the entropy weighting method to consumption data, POI, housing prices, and PM 2.5 concentrations, aiming to characterize various facets of spatial vitality including economic, cultural, residential, social, atmospheric, and nocturnal.

When multivariate data are utilized for assessing spatial vitality, the results obtained are more accurate and comprehensive than those obtained using evaluations based solely on a single data source. However, the inclusion of multiple variables, due to inconsistencies in data units, collection methods, and characterizations, may lead to difficulties in interpretation and information overload. Therefore, we propose our first research hypothesis: Quantifying urban vitality through both real and virtual perspectives could achieve vitality measurements that were closely related to neighborhoods and residents' daily lives.

2.2. The impact of the physical neighborhood environment on vitality

The physical environment provides space for daily human activities and social interactions, which serves as a crucial foundation for vitality (Yue et al., 2019). The 5D framework system proposed by Ewing and Handy (2009) has been widely used. Chen et al. (2023) argued that it was reasonable that density and diversity received the most attention because vitality depended on various human activities. Density variables associated with the macro-built environment encompass population density and building density (Liu and Li, 2022; Xia et al., 2020). Population density represents the concentration level of residents and

Table 1
Data sources and processing methods of existing vitality studies.

Variables	Data Sources	Data description and extraction	Refs.
Distribution of population density	Baidu heat map	The Baidu heat map updates every 15 minutes, providing real-time dynamic information about crowd distribution. A total of 53 Baidu heat maps were collected.	Li et al. (2019)
	The study obtained 41 heat maps with 3.5 m spatial resolution.		Lyu and Zhang (2019)
	Heat map data was collected at 60-minute intervals. The study utilized 34 heat maps with a 3.5-meter spatial resolution.		Fan et al. (2021)
Urban vitality	SKT measurement data	Density of resident population (person/m2).	Lee and Kang (2022)
	Tencent location data	The study aggregated Tencent location data at a 1-km grid level, using the count of location-sensing events per grid as a proxy for urban vibrancy.	Chen et al. (2022b, Wu et al. (2023)
	Mobile phone data from China Unicom Smart Steps	Mobile phone data obtained in November 2019. In order to reflect or visualize the dynamics of urban vitality, the day was divided into four periods.	Chen et al. (2023)
	Small catering businesses	The study counted the number of small catering venues, including snack stores, fast food establishments, tea houses/cafés, and bakeries.	Ye et al. (2018)
	SVI & Weibo check-in data	The street-view images were input into the ADE20K trained network. Six categories were combined. One-month record of Weibo data was collected.	Li et al. (2022)
	Catering businesses & Night light data	The study used small catering businesses to represent daytime vitality and night light data to represent night time vitality.	Zhang et al. (2021a)
	POI and Sina Weibo data	The check-in data from Weibo will be utilized to calculate the density of social media check-ins in the study area.	Pan et al. (2021)
	Weibo check-in data	The number of check-ins represents the popularity and attractiveness of the location for app users.	Huang et al. (2022)
	POI density, land function mix, and Weibo check-in density	All data were standardized to range between 0 and 100, given the same weight as each variable and then multiplied to obtain the vitality value.	Ou et al. (2021)
	Night light index, Weibo check-in data, cultural POI, and NDVI	The data represent economic, social, street culture, and ecological vitality, respectively. Comprehensive urban vitality was obtained using the entropy method.	Shi et al. (2023)
	Consumption data, POI, housing price, PM 2.5 concentration, night light radiation	The data represent economic, cultural, life, social, air, and nocturnal vitality. Comprehensive urban vitality was obtained using the TOPSIS method.	Liu and Shi (2022)
Nighttime vitality	Daily Lunar BRDF-Adjusted Nighttime Lights dataset	This study used NTL radiance from the Daily Lunar BRDF-Adjusted Nighttime Lights dataset (Black Marble—VNP46A2) as an urban vitality proxy.	Zhang et al. (2021b)
Virtual vitality	Cell phone data, bank card transaction data, and Wi-Fi access points	The study utilized three datasets from the Seoul Institute, SK Telecom, and South Korea's open data, representing social, economic, and virtual urban vitality, all standardized to the census block level.	Kim (2018)
	Weibo check-in data	With a spatial unit of 1 km x 1 km and a time unit of 2 hours, the check-in density for each spatiotemporal unit was calculated to serve as an indicator of vitality.	Jiang Haiyan (2023)
Economic vitality	Dianping	The study used Dianping comments to proxy consumer vitality, one of the main components of economic vitality.	Long and Huang (2019)
	Night light data	The study employed an auto-encoder model, integrating DMSP-OLS and NPP-VIIRS NTL data through convolutional neural networks, to extend the global annual NPP-VIIRS-like NTL series.	Sun and You (2023)

frequency of activities within the living environment. However, few studies have differentiated between settlements and other urban functional areas.

Regarding diversity, research indicates that land use diversity can potentially stimulate social interactions and commercial activities (Xia et al., 2020; Ye et al., 2018). Several studies have established that local spatial relationships of vitality are linked to land -use mix (LUM) (Long and Huang, 2019; Sung and Lee, 2015; Xia et al., 2020; Ye et al., 2018). Importantly, Xia et al. (2020) noted that existing research had not sufficiently addressed the distinctive features of various functional land uses. They highlighted the need to consider land-use functions. This argument underpins the selection of neighborhoods in our research.

Design variables are significantly correlated with spatial vitality. Previous studies have confirmed the importance of well-coordinated street architecture, appropriate aspect ratios, defined boundaries, spaces for leisurely walks, appealing landscaping, and well-kept amenities in creating thriving neighborhoods (Jacobs, 1993). Wu et al. (2022) further investigated the link between urban street design quality and vitality, revealing that the design directly and indirectly influences the vitality.

Destination accessibility has been established as a critical indicator of vitality. Efficient transportation infrastructure, superior location, and user-friendly street networks provide residents with more functionality and enhance spatial experiences (Chen et al., 2023; Wu et al., 2022; Yang et al., 2021a; Ye et al., 2018; Yue et al., 2019). Yue et al. (2019) revealed an inverse correlation between vitality and the distance from the city center, substantiated by their examination of three dynamic clusters in Shanghai.

Distance to transit is a fundamental attribute of the built environment. It has been characterized as the median distance to the nearest bus and metro stops (Lu et al., 2019; Wu et al., 2018).Scholars generally agree that convenient public transportation systems and walkable environments can promote social interaction.

These findings validate the macro-level connection between the physical environment and vitality. Therefore, we propose our second hypothesis: The observed positive correlation between urban vitality and factors such as public transportation efficiency and greening in the current study may also be applicable to residential area

2.3. The measurement of eye-level perceptions

2.3.1. Objective measurement of eye-level spatial features

Objective measurements of eye-level spatial features rely on the use of Street-View Images (SVIs) and semantic segmentation. Yin and Wang (2016) used pixel-level information to conclude that the sky constituted a significant measure of “enclosure”. Ma et al. (2021) used formulas to calculate the effects of openness, greenness, enclosure, walkability, and imageability on urban renewal. Based hereon, Qiu et al. (2023) explored the correlation between street-view perceptions and housing prices. Wu et al. (2023) calculated building continuity, thereby elucidating the importance of urban interface continuity in enhancing vitality. Their method involved calculating the standard deviation of the proportion of buildings in a grid. A subsequent study improved on the existing formula by questioning the covariance of openness and enclosure and using it to measure the impact of greenness, enclosure, walkability, and imageability on street accessibility (Rui, 2023b).

However, there are limitations to the formula-based objective measured eye-level features. For instance, the computation of building continuity via standard deviation within a grid overlooks the continuity of building facades in adjoining grids. Additionally, objective eye-level features extracted from an SVI cannot comprehensively represent residents’ overall perception of the environment (Ewing and Handy, 2009).

2.3.2. Subjective measurement of eye-level perceptions

In 2013, the Massachusetts Institute of Technology (MIT) Media Lab launched Place Pulse, including wealthy, beautiful, safe, boring, lively, and depressing perceptions. Subjective eye-level perceptions were used to explicate the relationship with housing prices (Qiu et al., 2023; Qiu et al., 2022), urban renewal (Ma et al., 2021; Qiu et al., 2021), and running (Dong et al., 2023). However, a scarcity of studies employing subjective perception to investigate NV are scarce. Moreover, Qiu et al. (2022) indicated that Place Pulse used United States-based (US-based) urban scenes and was not suitable for evaluating Chinese urban landscapes. In this regard, they developed their own subjective perception dataset and utilized 300 randomly selected SVIs from Shanghai to survey 43 participants (Qiu et al., 2021; Qiu et al., 2023; Qiu et al., 2022). However, the small sample size and participants may not capture the actual perceptions, while the random image selection method cannot guarantee that all types of streets are covered in the training set.

Based on the findings concerning both objective and subjective eye-level perceptions and the physical neighborhood environment, we introduce our third research hypothesis: Eye-level spatial measurements can supplement and amplify the relationship between the physical environment and NV. This bottom-up measurement approach can facilitate resident-centered neighborhood-planning strategies.

3. Data and methodology

3.1. Study area

Shenzhen was chosen as our study area (Fig. 1). The city can be broadly categorized into the core areas comprising Nanshan, Futian, and Luohu; the suburban areas encompassing Bao’an, Longhua, Yantian, and Longgang; and the outlying suburbs spanning Guangming, Pingshan, and Dapeng. Shenzhen accommodates a total of 1,877 UVs, with a population of 12 million residents, primarily comprising migrant populations (Rui, 2023a). In 2019, the Shenzhen Planning and Natural Resources (2019) introduced the “Shenzhen Urban Village Comprehensive Improvement Plan (2019–2025)” to revitalize the UVs by integrating supporting facilities and implementing functional changes.

We created a hexagonal study unit with each side measuring 200 meters. We defined the unit as an UV when the area of UV buildings was larger than that of an FN. Data on UV’s areas-of interest (AOIs) and the building data from OpenStreetMap (OSM) were obtained in February 2023. In Fig. 1, UVs are distinguished by the color red, constituting a total of 9,704 units (35.1 %). Conversely, FNs are depicted in yellow, comprising a total of 17,942 units (64.9 %).

3.2. Analytical framework and data sources

Our study is structured into four stages (Fig. 2). First, the Baidu heat map and Weibo check-in data were obtained for real and virtual vitality. Using entropy method, we derived comprehensive NV values. The second stage involved a quantification of the physical environment and eye-level perceptions. We employed the 5D framework for the physical-environment analysis. Instead of applying Place Pulse, we collected 100 sets of subjective-perception questionnaires, each containing 2000 SVIs, and used eXtreme Gradient Boosting (XGBoost) for predictions. Third, we tested for the correlations among all the variables and used Stepwise Regression (SWR) model to filter them out. We used Moran’s I to test for spatial autocorrelation and the Geographically and Temporally Weighted Regression (GTWR) model to explore the spatio-temporal relationships. Next, to resolve the bias induced by prematurely assuming a linear relationship in SWR (Yang et al., 2021a), we employed XGBoost to train and predict all the variables, and used Partial Dependence Plots (PDPs) for visualization. Fourth, this study proposes differentiated planning suggestions to support urban transformation.

This study drew on seven types of data, including Baidu heat map data, Weibo check-in data, POI, NDVI, and city map data (including administrative districts, streets, and building footprints), and population data (Table A1).

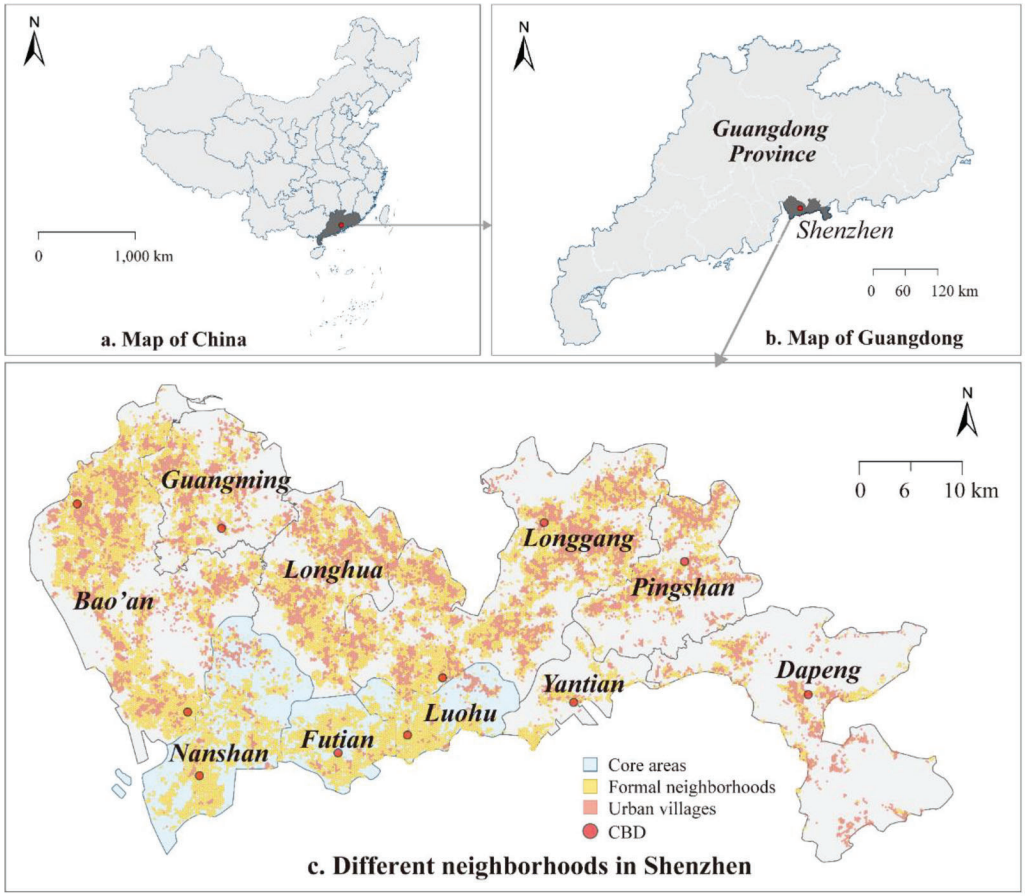

Fig. 1. Study area.

3.3. Calculation of neighborhood vitality

Baidu Heatmap, utilizing real-time geolocation data provided by smartphone users when using Baidu products, calculates the pedestrian activities in different urban areas. It characterizes the dynamic distribution of the population in urban spaces (Fan et al., 2021; Li et al., 2019; Lyu and Zhang, 2019). Therefore, we used Baidu Heatmap to represent the real vitality values of neighborhoods. We collected Baidu Heatmap data from Shenzhen on April 29 and 30, 2023, which were Saturday and Sunday. During the hours (6:00 to 24:00), heatmap data were collected every 30 min. In total, 76 heatmaps with a spatial resolution of 3.5 m were used. The real vitality values in this study are the average of different periods during the weekend.

To further characterize the virtual vitality, we collected Weibo check-in data from the same weekend. Mobile users share their location information on the internet via the Weibo platform, providing numerous check-in records (Pan et al., 2021). The check-in data can reflect the attractiveness and popularity index of urban places to virtual network users (Li et al., 2022). It embodies the deep integration of digital media with urban geographic elements and can be used to characterize the heat of cyberspace, i.e., the virtual vitality of the city (McQuire, 2017; Wang, 2019). On April 29, 2023, we acquired Weibo check-in data (https://open.weibo.com/wiki/API) from previous three months specifically focusing on weekends. The texts shorter than 5 characters and longer than 150 characters were excluded. Additionally, we filtered the records based on the geolocation information provided, omitting those outside residential areas. We obtained a total of 108,028 Weibo check-in records.

We chose the entropy method to calculate NV. The entropy method for determining weights is based on the data itself, avoiding subjectivity that may arise in weight determination (Lan et al., 2020; Zhou and Luo, 2017). The weights assigned to real and virtual vitality are 30.997 % and 69.003 % respectively.

3.4. Physical neighborhood environment

Based on the 5D framework, we re-screened the variables of the physical neighborhood environment (Table 2). Descriptive statistics for all variables and the classification criteria for POI are presented in Table A2.

3.5. Objective eye-level features

SVI allows for observing the urban environment from an eye-level perspective. Baidu Map provides APIs that enable users to download SVI data in bulk. We established sampling points at 50 m intervals on the road network (Fig. 3), and a total of 119,621 sample points were obtained. SVIs were obtained using an HTTP URL. To represent the residents' perspectives, for each sample point, data from four directions (headings of 0°, 90°, 180°, and 270°) were collected on May 1, 2023. The vertical angle (pitch) was set at 20°, with the field of view (fov) adjusted to a width of 90°. By combining perspectives from the four directions, a panoramic street view was created for each sample point. The camera equipment and resolution of the photos (600 × 400 pixels) were kept consistent. From the 119,621 sample points, a total of 119,052 valid data points were obtained.

We selected the following spatial characteristics: greenness, openness, enclosure, walkability, imageability, and building continuity (Ma et al., 2021; Rui, 2023b; Wu et al., 2023). To compute objective spatial features, we employed DeepLab V3+ and integrated it with ADE20K as a pre-trained dataset for training and prediction based on our sample

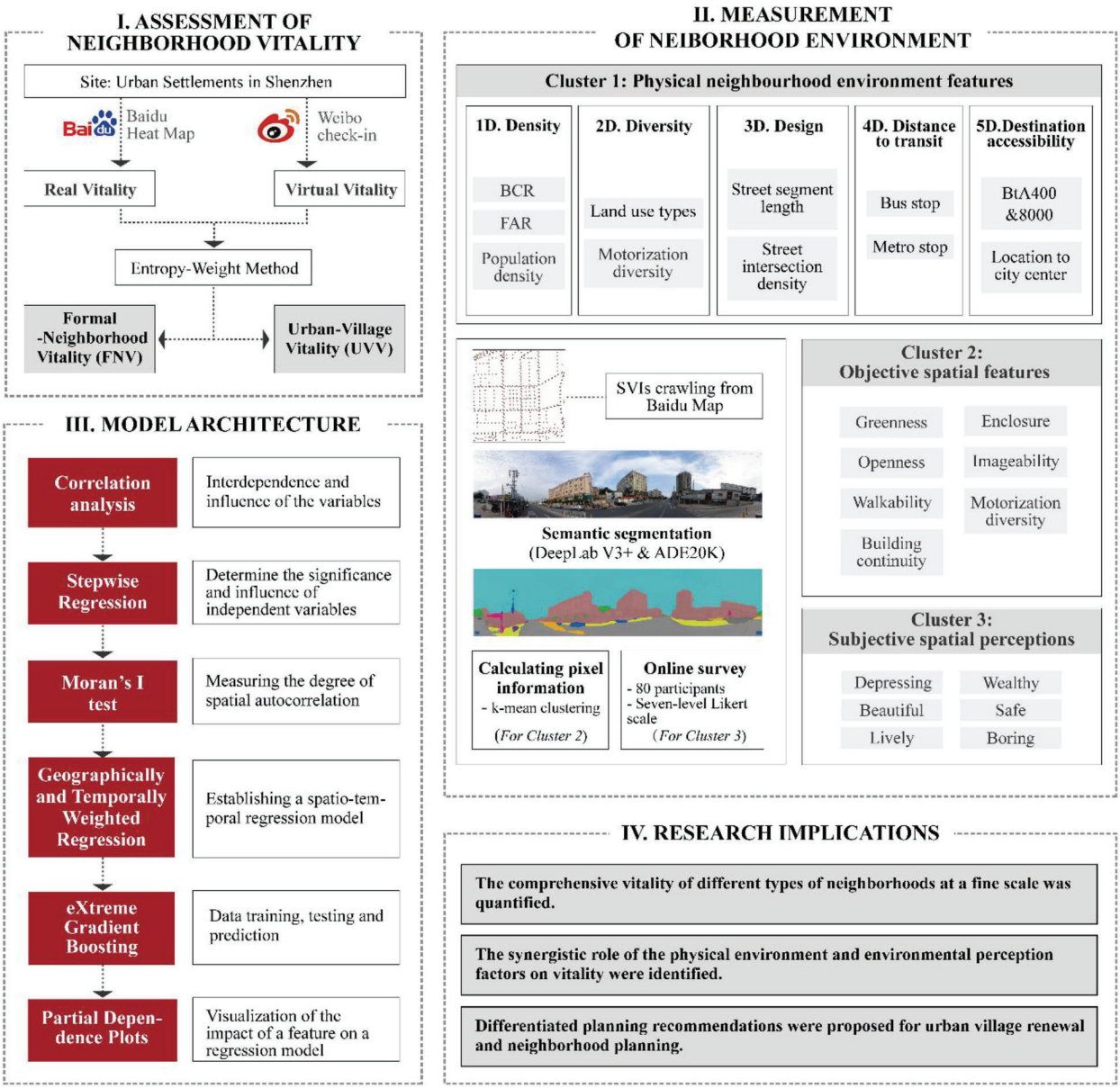

Fig. 2. Analytical framework.

Table 2
Definitions and calculations of 5D variables.

Clusters	Variables	Definitions and calculations
1D: Density	BCR	The ratio of the total standing area of all buildings to the total area of the grid. $BCR = B/A$ (Eq. 1) Where B and A denote are the gross building footprint (km^2) and gross area (km^2).
	FAR	The ratio of the gross floor area of all buildings to the total area of the grid. $FAR = F/A$(Eq. 2) Where F and A denote are the grass floor area (km^2) and gross area (km^2).
	Population density	The WorldPop dataset provides gridded population maps with a 100-m spatial resolution for each country in the dataset.
2D: Diversity	LUM	The degree to which those different types of land uses are physically and functionally integrated. $LUM = -\sum(P_i)(\log P_i)$ (Eq. 3) Where P_i the ratio of the i^{th} land type to the total area.
	Residence, commerce, industry, greenspace, public service, transportation services	Land use is classified into six dummy variables (Li et al., 2018). By Dong et al. (2023), if a specific type of point of interest (POI) exists in the study unit, it is assigned a value of 1; if not, it is assigned a value of 0.
3D: Design	Street segment length	The total length of streets within each study unit, is measured in meters.
	Intersection density	The number of street intersections within each study unit.
4D: Distance to transit	Bus stop	The distance from each study unit to the nearest bus stop (unit: meter).
	Metro stop	The distance from each study unit to the nearest metro stop (unit: meter).
5D: Destination accessibility	BtA400 BtA8000	Street accessibility measurements were conducted using Spatial Design Network Analysis (sDNA) (Chiaradia, Cooper, & Webster, 2012). Betweenness analysis evaluates the potential of each street unit to serve as a preferred pedestrian pathway, reflecting its "through-movement" potential (Al_Sayed et al., 2014). It predicts the most easily accessed streets at the study area. Refer to Cooper and Chiaradia (2020), we selected 400 m as a comfortable walking distance. Based on the "Commuting Monitoring Report for Major Cities in China" (China Academy of Urban Planning and Design, 2022), we chose 8000 m radius as automobile distance: $C_b(P_i) = \sum_{j=1}^{n}\sum_{k=1}^{n} g_{ik}(p_i)/g_{jk}(j<k)$ (Eq. 4) where $g_{ik}(p_i)$ is the number of geodesics between node p_j and p_k that contain node p_i, and g_{jk} is the number of all geodesics between p_j and p_k.
	Location to city center	We chose the Shenzhen government as the city center and calculated the linear distance (meters) from the center of each study unit to the city center.

observations. Table 3 shows the formulas and explanations of objective eye-level features.

3.6. Subjective eye-level perceptions

We trained and predicted our dataset based on the samples we collected. We utilized the K-means clustering algorithm to segment all the samples observations, better capturing SVI characteristics. Categories that constituted less than 0.1 % of the semantic segmentation results were filtered out, resulting in 19 categories (Fig. 4a.1). We set the value of k to 5 based on the elbow method to accommodate the variety in street types (Fig. 4a.2). Five categories were characterized by the visual elements of sky, sky & building, tree, sky & tree, and building (Fig. 4a.3 and a.4).

In April 2023, we invited 100 participants to view SVIs and rate them based on subjective eye-level perceptions. The participants aged between 21 years and 35 years (48 males, 52 females). The average age of the participants was 27.5, with a standard deviation of 3.79. Before scoring, each participant was required to confirm that they had normal vision and signed a consent form indicating their voluntary participation. We used a 7-point Likert scale to evaluate perceptions (Fig. 4b.1 and b.2). Within the Likert scale, lower values indicate weaker perceptions, while higher values suggest stronger perceptions. Fig. 4c displays the average ratings for "beautiful" after various participants assessed different urban spaces. Finally, using the same 19 semantic segmentation indicators from the K-means clustering as independent variables, we built predictive models for the six indicators using XGBoost and predicted scores for all the SVIs (Table A4).

3.7. Model architecture

3.7.1. SWR, spatial autocorrelation, and Moran's I

SWR iteratively chooses independent variables for linear regression, offering automatic feature selection and enhanced model clarity. In SWR, we set the criteria such that variables with a *p*-value less than 0.05 are included, while those with a *p*-value greater than 0.1 are excluded. The global Moran's I examines spatial correlation patterns across the study area (Moran, 1950). We further conducted a local analysis of the dependent variable to identify and assess spatial autocorrelation within individual areas. We employed local Moran's I, also known as the Local Indicator of Spatial Association (LISA), to evaluate the statistical significance of spatial disparities.

3.7.2. GTWR

GTWR is a geographically weighted technique that optimized upon the GWR model (Huang et al., 2010). By incorporating the temporal dimension, it accounts for both spatial and temporal heterogeneity.

$$Y_i = \beta_0(u_i, v_i, t_i) + \sum_k \beta_k(u_i, v_i, t_i)X_{ik} + \varepsilon_i \quad (7)$$

Here Y_i denotes the explanatory variable of point i (coordinates of UVs and FNs), u_i and v_i represent the space longitude and latitude coordinates of point i, while t_i corresponds to the time coordinate. (u_i, v_i, t_i) represents the space-time dimension coordinate of point i. Furthermore, $\beta_0(u_i, v_i, t_i)$ together is the intercept value of point I and $\beta_k(u_i, v_i, t_i)$ denotes the regression coefficient of explanatory variable k at point i; X_{ik} is the explanatory variable k at point i; ε_i is counted as random error.

3.7.3. XGBoost and partial dependence plots (PDP)

XGBoost is a optimized machine learning algorithm proposed by (Chen and Guestrin, 2016), which is based on decision trees and uses Classification and Regression Trees (CART) to classify and predict datasets. In this study, XGBoost is primarily used for training and predicting the independent and dependent variables.

The PDP technique is able to reveal the impact of specific factors on the prediction results of machine learning models. By visualizing the marginal effects of features, PDPs enable researchers to review the relationships between variables. The partial dependence function is expressed as follows:

$$\widehat{f}_{x_S}(x_S) = E_{x_C}[\widehat{f}(x_S, x_C)] = \int \widehat{f}(x_S, x_C)d\mathbb{P}(x_C) \quad (8)$$

Each variable S has its own partial dependence function that can be

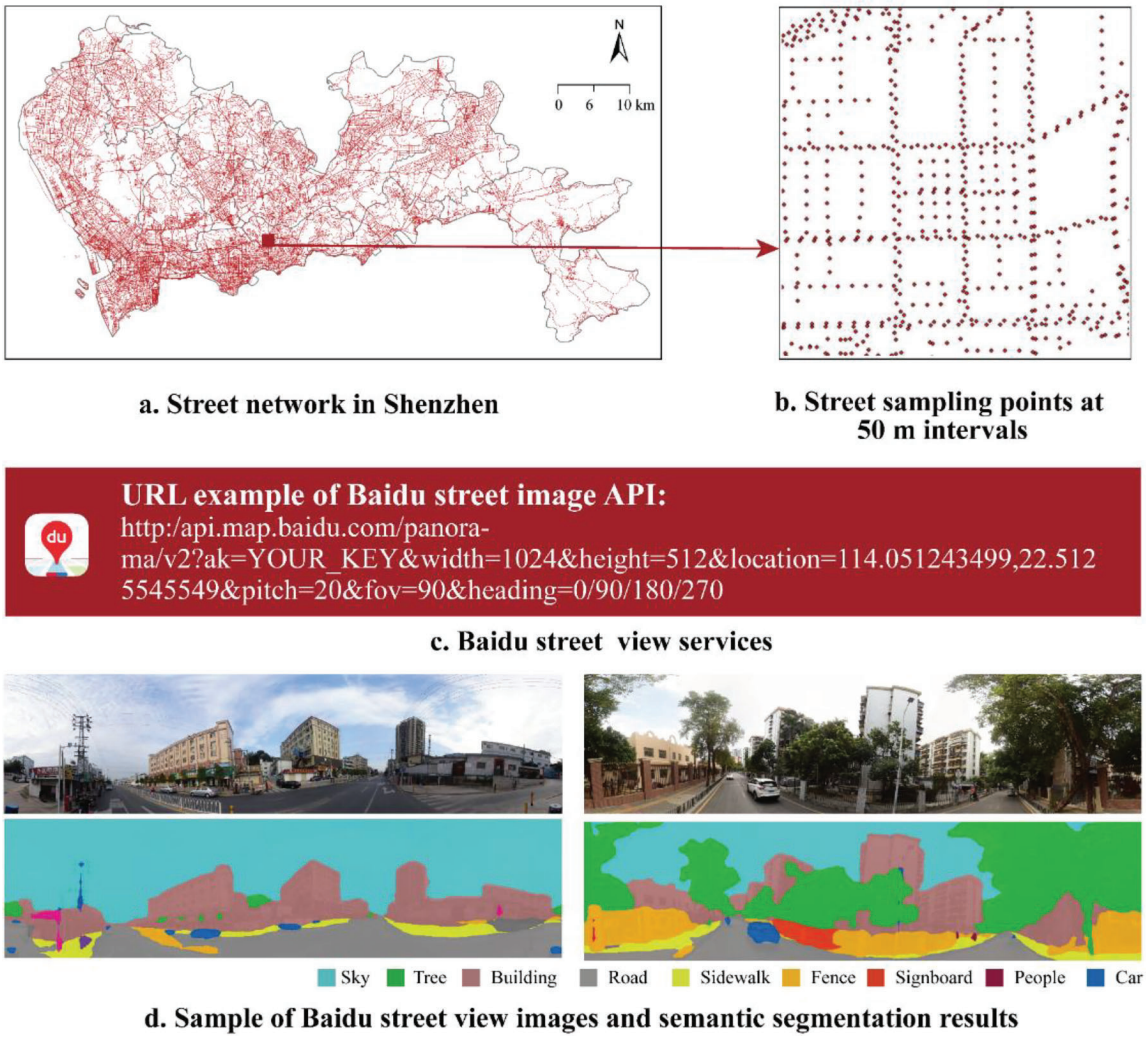

Fig. 3. Example of the SVIs collection process and semantic segmentation.

calculated as the mean where is held fixed and varies over its marginal distribution. This makes both and uncertain. Therefore, we applied the Monte Carlo method to calculate (Eq. 8) in order to estimate (Eq. 9):

$$\widehat{f}_s = \frac{1}{N}\sum_{i=1}^{N}\widehat{f}(x_S, x_{C_i}) \tag{9}$$

The value of the training data x_c is represented by $\{x_{C_1},\ldots,x_{C_N}\}$. When dealing with multiple classes, PDP plots the results using a pairwise residual method.

4. Results

4.1. Spatial temporal patterns of NV

This study undertakes a detailed segmentation analysis of the temporal dimension. We subdivide the day from 6 a.m. to midnight into five intervals, intentionally excluding the sleep hours from midnight to 6 a.m. Specifically, we designate 6 to 9 a.m. as "Early Morning," 9 a.m. to 1 p.m. as "Morning," 1 to 7 p.m. as "Afternoon," 7 to 10 p.m. as "Evening," and 10 p.m. to midnight as "Night." This temporal segmentation allows us to delve deeper into the variations in residential vitality across geographical and spatial dimensions, thereby laying a solid foundation for the application of the GTWR model.

Table 3
Formulas and explanations of objective eye-level features.

Variables	Formulas	Explanations
Openness Greenness Enclosure Walkability Imageability	Openness = S_i Eq. 5 (Rui, 2023b)	S_i denotes the proportion of sky pixels.
Building continuity	*Building continuity* = $1-\lvert B_i-\overline{B_i}\rvert$ Eq. 6	B_i denotes the proportion of building pixels, $\overline{B_i}$ denotes the average of building pixels on the road where the point is located.
Motor vehicle diversity	We used the VOLOv7 (Yuan et al., 2022) to identify the presence of bicycles, cars, motorcycles, buses, and trucks in each SVI. By summing up these values, we determined the total count of each vehicle type and employed the inverse distance weight method for calculation.	

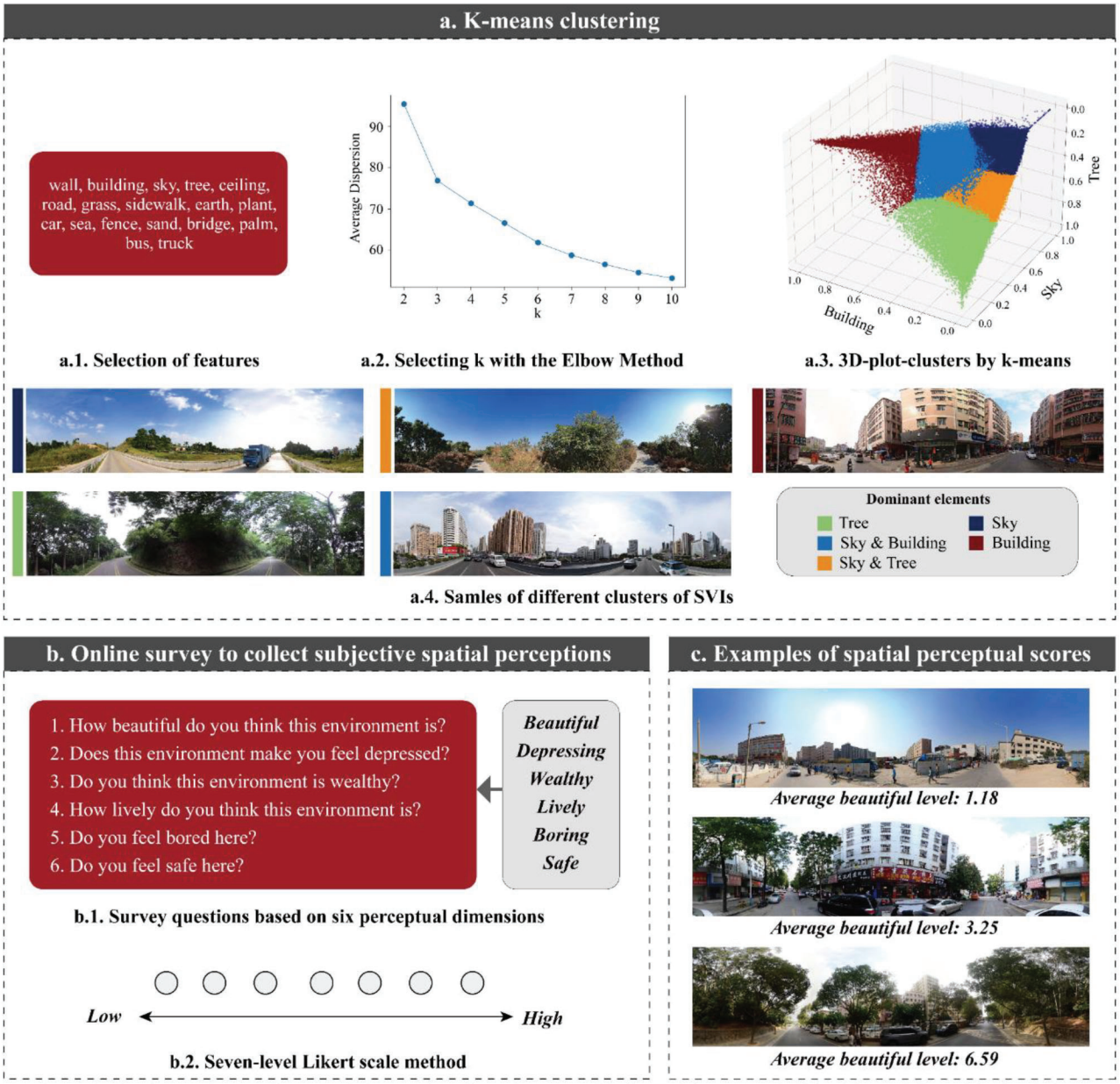

Fig. 4. The procedure of measuring the subjective spatial perceptions.

Fig. 5 illustrates the NV in Shenzhen. The temporal pattern reveals a general increasing trend of vitality from morning to night. The spatial pattern explicitly identifies higher values concentrated within core areas, with scattered clusters in the central and southern areas of Longhua and southern part of Bao'an. The Urban Village Vitality (UVV) ranges from 0.310 to 464.305, while the Formal Neighborhood Vitality (FNV) ranges from 0 to 1,741.992. This indicates that the vitality of FNs is higher than that of UVs. At the district level, the core areas have the highest average vitality in the early morning and morning, while the suburbs are higher in vitality in the afternoon and evening.

Fig. 6a and 6b provide preliminary confirmation of the first research hypothesis, indicating noticeable trends and temporal variations in both real and virtual vitality, suggesting that compared to a single data source, a more comprehensive assessment can be achieved. The real vitality in all the neighborhoods reveals that most residents' physical activities are primarily clustered between 9 a.m. and 21 p.m. Few peaks occur in the morning (11–12 a.m.) and afternoon (17-18 p.m.) (Fig. 6a). In contrast to the real vitality, the virtual vitality presents a stable increase throughout the day, reaching its peak at midnight (Fig. 6b). Moreover, the daily dynamics of UVV and FNV are similar, with a noticeable growth in the early morning, stable increase in the morning, slight decrease in the afternoon, and continued growth in the evening until a decline at night. The peak appears between 9 p.m. and 10 p.m. (Fig. 6s c and d).

4.2. Model results

4.2.1. SWR results

The SWR model achieved R^2 values of 19.2 % and 51.2 % in FNs and UVs respectively, suggesting that the variables selected in this study had a stronger explanatory power for UVV than for FNV. The variance inflation factor (VIF) for all the variables was less than 7.5, indicating no multicollinearity. As the SWR includes a filtering step, all the variables shown in Table A5 are suitable for the GTWR.

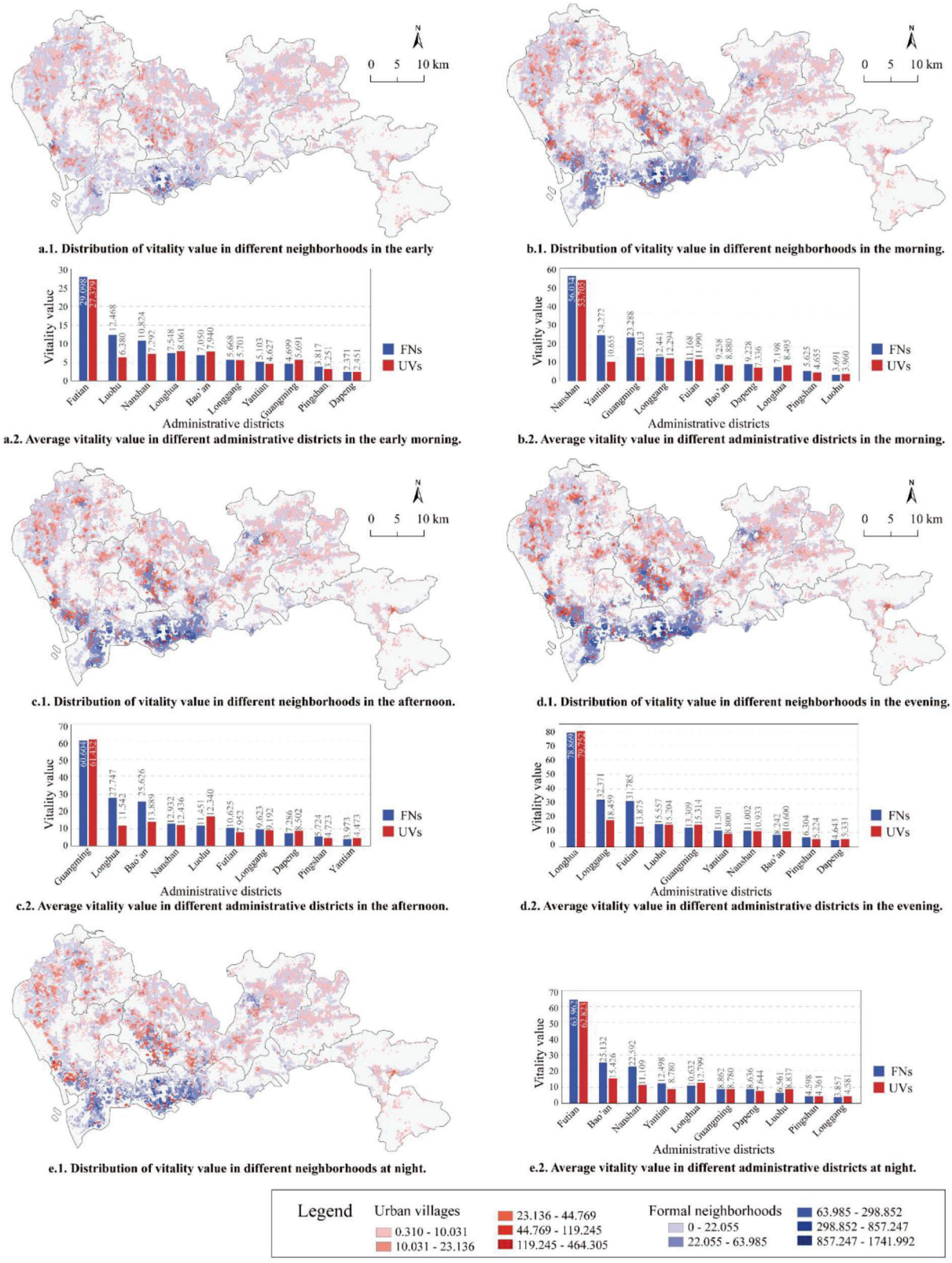

Fig. 5. Distribution of neighborhood vitality value in FNs and UVs at different time periods.

4.2.2. Spatial cluster of neighborhood vitality

Fig. 7 presents the Moran's I index for NV from early morning to night: 0.758, 0.903, 0.939, 0.936, and 0.467. These results are significant ($p < 0.001$), emphasizing a positive spatial dependence and a spatial clustering effect. The map reveals clear hot and cold spots in NV. The hot spots (high-high clusters) have a stable distribution throughout all time periods. These are concentrated in the city center, as well as in suburban locations such as the southern parts of Bao'an and Longhua and southwestern and central parts of Longgang. Conversely, the cold spots (low-Low clusters) predominantly occupy the outlying suburbs,

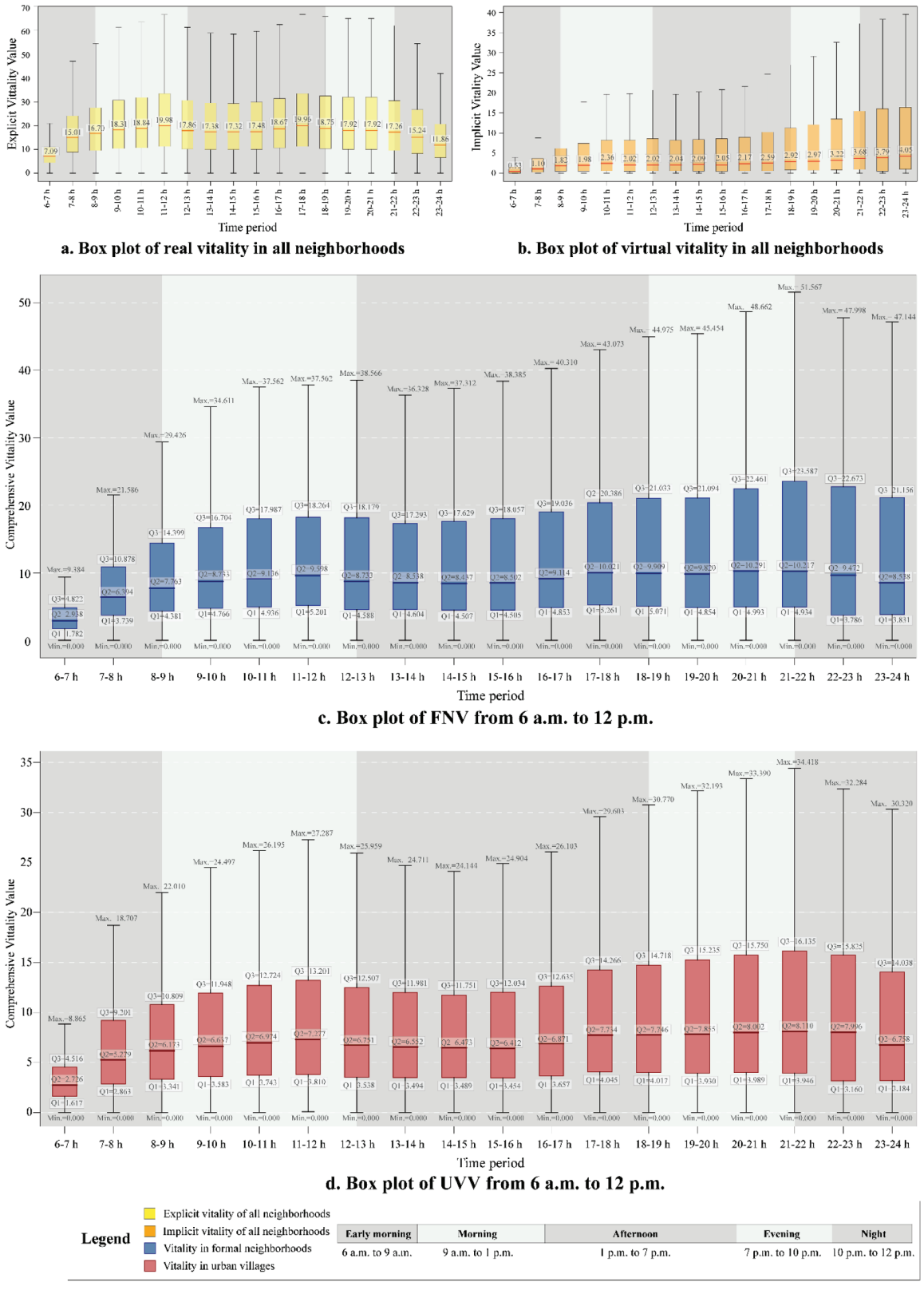

a. Box plot of real vitality in all neighborhoods

b. Box plot of virtual vitality in all neighborhoods

c. Box plot of FNV from 6 a.m. to 12 p.m.

d. Box plot of UVV from 6 a.m. to 12 p.m.

Fig. 6. Box plots of different vitality in FNs and UVs.

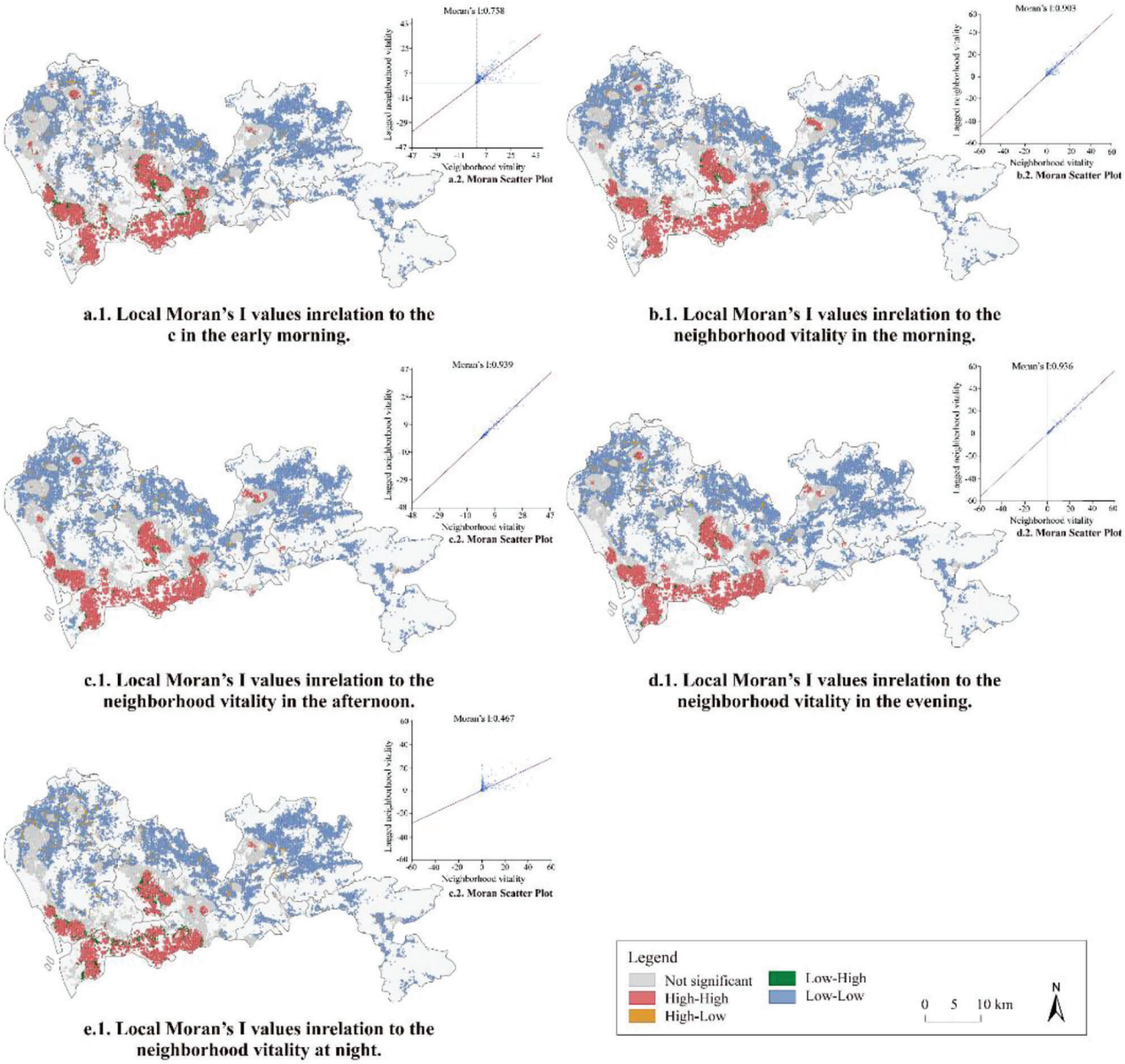

Fig. 7. The LISA cluster maps displayed local Moran's I value in relation to the neighborhood vitality values.

Table 4
Comparison of model performance on neighborhood vitality at different time periods in FNs and UVs.

FNs	SWR				GTWR			
	R^2	Adj. R^2	AIC	AICc	R^2	Adj. R^2	AIC	AICc
Early morning	0.202	0.201	46914.518	46916.565	0.705	0.642	35359.916	36729.561
Morning	0.185	0.184	47283.261	47285.308	0.823	0.769	28273.651	30858.815
Afternoon	0.174	0.173	47535.230	47537.277	0.833	0.782	27179.569	29764.733
Evening	0.140	0.140	48239.094	48241.141	0.820	0.764	28603.888	31189.052
Night	0.106	0.105	48947.531	48949.578	0.325	0.280	46096.009	46242.253
UVs	SWR				GTWR			
	R^2	Adj. R^2	AIC	AICc	R^2	Adj. R^2	AIC	AICc
Early morning	0.526	0.526	20322.693	20324.780	0.805	0.773	14390.688	14839.914
Morning	0.521	0.520	20434.057	20436.144	0.807	0.777	14162.706	14558.864
Afternoon	0.500	0.499	20857.961	20860.047	0.808	0.778	14128.222	14524.380
Evening	0.479	0.478	21255.367	21257.454	0.794	0.762	14799.307	15195.464
Night	0.467	0.466	21477.690	21479.776	0.775	0.745	15317.283	15609.600

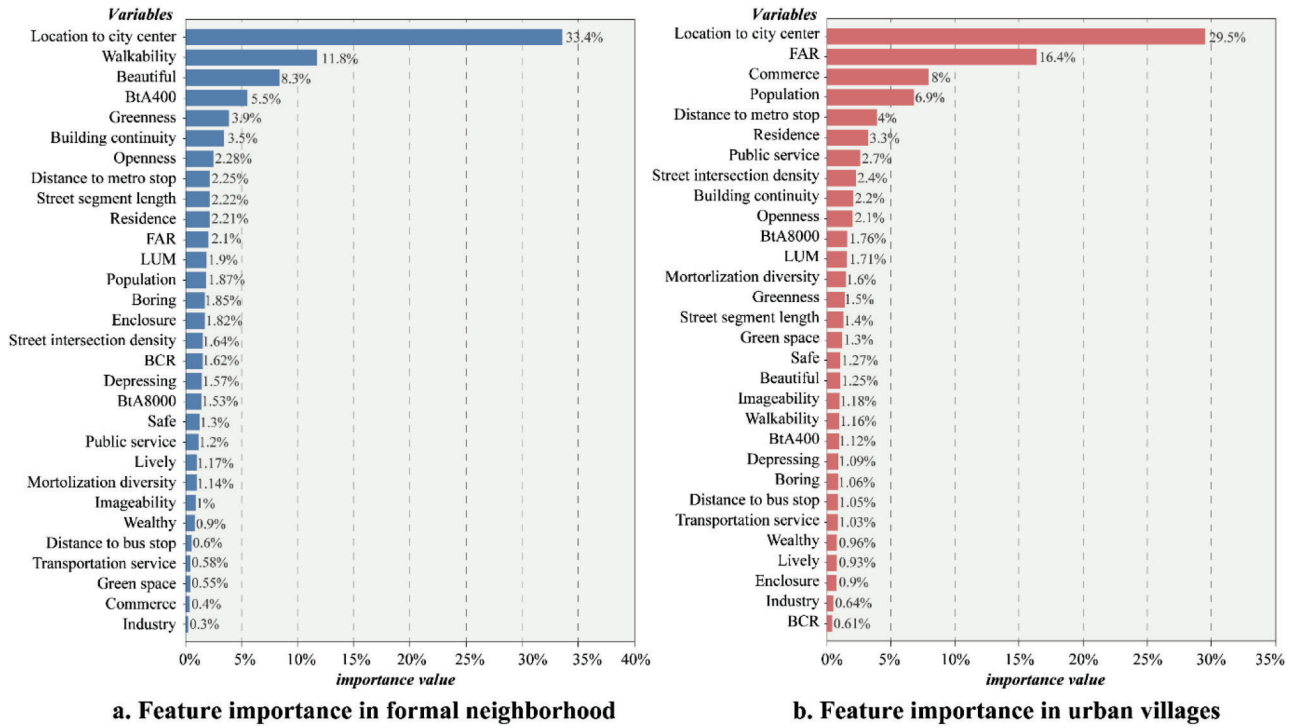

Fig. 8. Feature importance in formal neighborhoods and urban villages.

suggesting a positive correlation with the distance from the city center.

4.2.3. GTWR results

Table A6 demonstrates that the selected variables exhibit strong spatial autocorrelation, which is applicable to GTWR. An adaptive bisquare spatial kernel is employed in GTWR models to distinguish between global and local effects across different time periods. The corrected Akaike Information Criterion (AICc) was utilized as the determining parameter for optimization, with the golden section facilitating bandwidth searching. GTWR models reveal the heterogenous relationships between variables at different spatial locations and time points. Table 4 indicates that the GTWR models outperformed the SWR models, as reflected by the higher R^2. Furthermore, the AIC and AICc in the GTWR models were smaller than those in the SWR models, underscoring the former models' superior capacity for data explanation.

4.2.4. XGBoost results

The selection of XGBoost was determined based on its performance in managing this study's dataset. We employed six machine-learning models for training based on our data and to predict the results and found that XGBoost outperformed the others in all aspects (Table A7). We divided the XGBoost dataset into an 80 % training set and a 20 % testing set, implementing a learning rate of 0.001 and a tree complexity of 10. The R^2 values for FN and UV are 0.618 and 0.760, respectively. In FNs, the RMSEs for the training and testing sets, as processed through XGBoost, both reach 0.004; in contrast, the RMSEs in UVs are 1.276 and 3.127, respectively. The relatively small RMSEs underscore a minimal discrepancy between the observed and predicted values, indicating a high degree of predictive accuracy.

Fig. 8 shows the ranked importance of variables impacting the NV. Noticeabley, "location to city center" stands as the most influential variable across all neighborhoods. In FNs, walkability, beautiful, and BtA400 are the second-, third-, and fourth-most influential variables, respectively. This implies that variables such as the percentage of sidewalks and pedestrian accessibility play a crucial role in enhancing FNV, while a beautiful neighborhood environment can attract residents. However, the results in UVs are different from those in FNs. FAR, commerce, and residential density ranki second, third, and fourth, respectively. These findings corroborate our initial hypotheses, given the high-density characteristic of UVs and substantial influence of FAR and residential density. The presence of commerce also indicates the location of an UV and convenience of employment for the UV residents.

4.3. Joint analysis

4.3.1. Physical environment on neighborhood vitality

a. Location to city center and FNV

A one-way PDP shows a noticeable declining trend (Fig. 9a.6), indicating that the closer to the city center, the higher the vitality. A two-way PDP indicates that population density and FAR contribute to more vitalitycloser to the city center (Fig. 9s.a.8 and a.9). Residents are the cornerstone of NV (Wu et al., 2023), and high-density residential areas can accommodate more residents, thus showing a positive correlation with vitality. Moreover, we found that walkability did not significantly impact location to the city center and NV (Fig. 9a.7). Considering the scale of Shenzhen and average commuting distance (8 km), it is difficult to rely on walking to reach the city center. GTWR indicates that walkability exhibits a negative correlation with the distance to the city center and vitality in core areas (Fig. 9s.a.1 to a.5). In contrast, a positive correlation is observed in other city areas. Interestingly, location to city center in the morning (excluding the core areas) and night shows the highest positive correlation.

b. Location to city center and UVV

A two-way PDP indicates that the proximity of UVs to a metro enhances vitality (Fig. 9b.10). Notably, when the correlation coefficient of location to city center is relatively low (coefficient between 0.2 and 0.35 after standardization), the furthest distances from the metro stop (>0.13, corresponding to distances above 1200 meters) demonstrate the lowest UVV values (0.02) (Fig. 9b.8). In other words, for residents living in UVs relatively close to the city center, if the distance to the metro stop

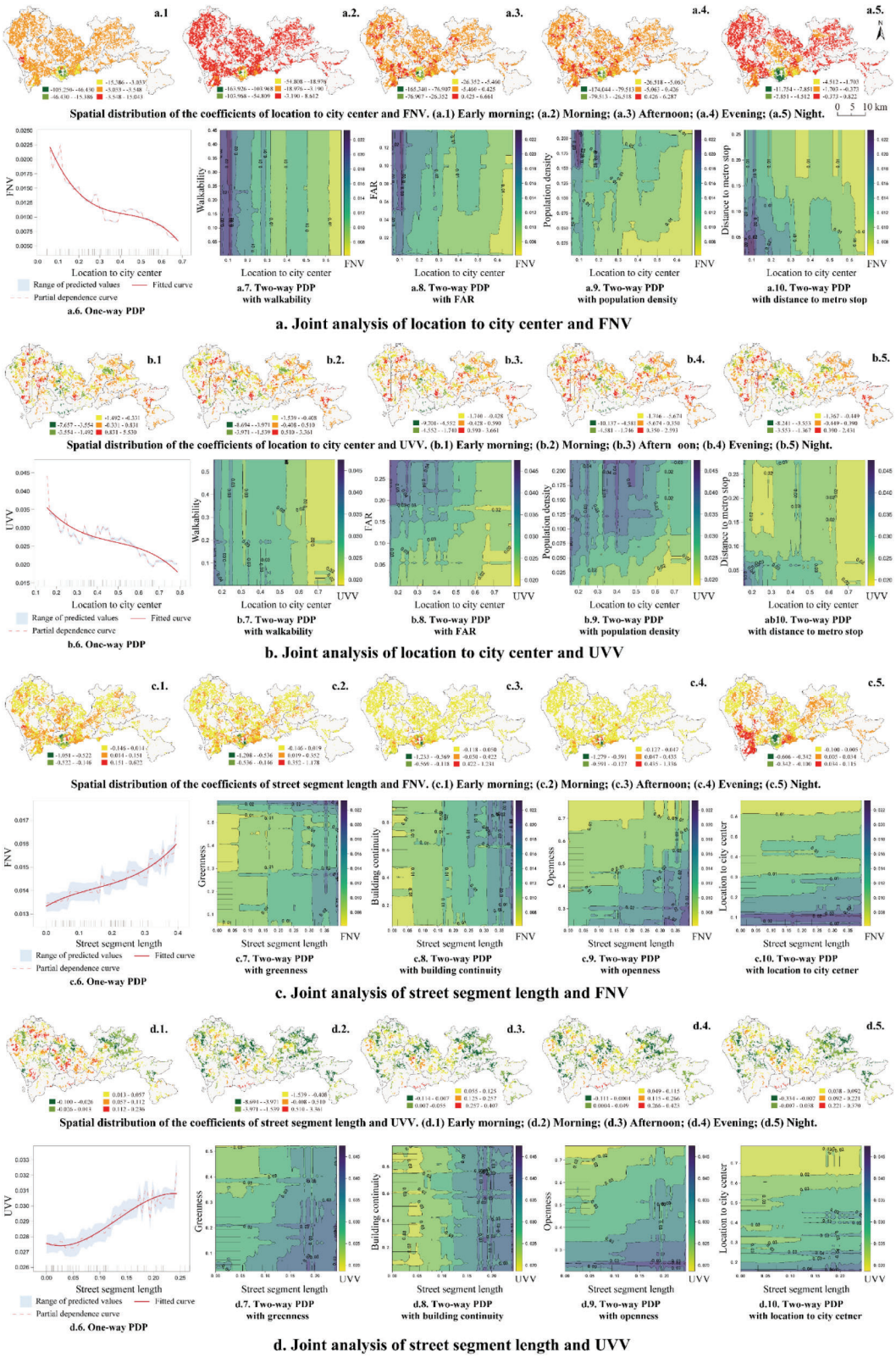

Fig. 9. Joint analysis of variable cluster I on FNV and UVV.

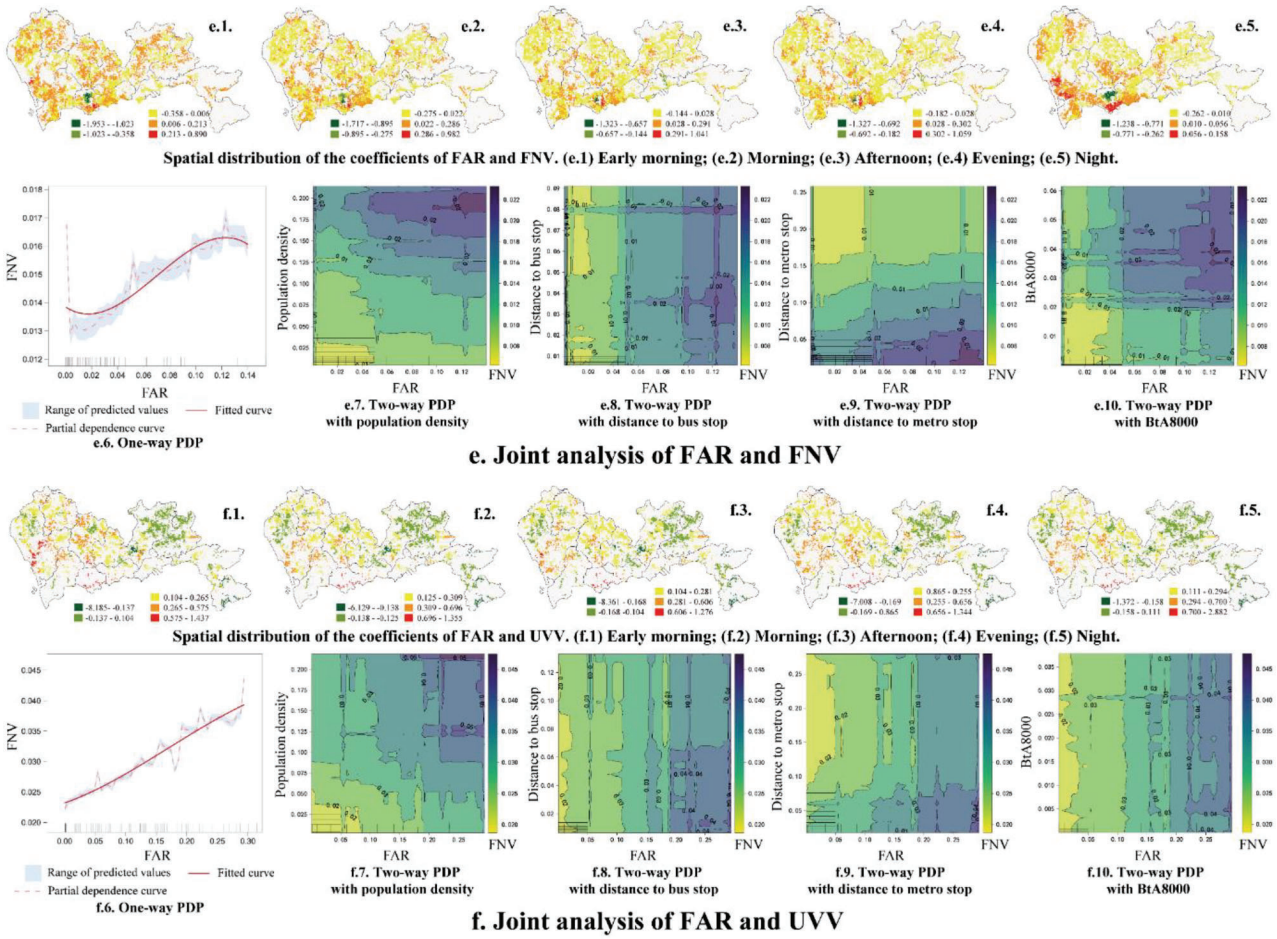

Fig. 9. (*continued*).

exceeds an acceptable range (above 1200 meters), it is detrimental to the generation of NV.

In GTWR, FNs show strong spatial autocorrelation, while UVs display clear spatial heterogeneity, with high and low values dispersed inconsistently (Fig. 9s.b.1 to b.5). Areas with high positive correlation to the location to city center are scattered across various positions within each administrative district. In Fig. 9b.9, we found that areas with high UVV (>0.04) were also distributed when the coefficient of location to city center was between 0.2 and 0.5, and the population density coefficient exceeded 0.2. This is consistent with the findings from the GTWR, indicating that a higher population density in UVs contributes to reducing their dependence on distance to the city center. This highlights the unique characteristics of UVs as "mini economic zones", which play an encouraging role in promoting regional circulation and fostering the formation of polycentric urban structure (Rui, 2023a).

c. Street segment length and FNV

A one-way PDP indicates a positive correlation between street segment length and FNV (Fig. 9c.6). A two-way PDP shows that an increase in greenness helps to enhance this relationship (Fig. 9c.7). Areas with high FNV (>0.02) are distributed when the street segment length coefficient is between 0.33 and 0.35. This suggests that more greenery in FNs can bring more vitality and reduce dependence on street density (Gupta et al., 2012). The contribution of openness to the relationship between street segment length and FNV is negative (Fig. 9c.9). High-FNV areas concentrate in places with lower openness (<0.4). Less openness can enhance residents' sense of security and willingness to walk (Singh, 2016). Another factor that plays a negative role is location to the city center (Fig. 9c.10). Noteworthily, that this relationship is not linear, as high FNV occur at a location-to-city-center coefficient of 0.1, not 0. This indicates that high-vitality FNs are concentrated around the city center. Low values in the core areas from the GTWR results further support this finding (Fig. 9c.1 to c.5).

d. Street segment length and UVV

The relationship between street segment length and UVV presents a nonlinear relationship that first decreases and then increases (Fig. 9d.6). A lower street segment length contributes weakly to UVV. That the correlation coefficients for street segment length across five time periods were dispersed in the distant suburbs (Fig. 9d.1 to d.5) was supported by the GTWR results. A two-way PDP shows different results from those

Table 5
Population and area data for administrative districts.

	Population (count)	Area (km^2)	Ratio (count/km^2)	Ranking
Futian	1,553,225	78.8	19,710.977	1
Luohu	1,143,801	78.36	14,596.745	2
Longhua	2,528,872	175.58	14,402.961	3
Bao'an	4,476,554	398.38	11,236.894	4
Longgang	3,979,037	387.82	10,260.009	5
Nanshan	1,795,826	182	9,867.175	6
Guangming	1,095,289	155.45	7,045.924	7
Pingshan	551,333	167.01	3,301.197	8
Yantian	214,225	72.36	2,960.544	9
Dapeng	65,663	295.06	222.541	10

Data source: The seventh national census of Shenzhen (http://tjj.sz.gov.cn/zwgk/zfxxgkml/tjsj/tjgb/content/post_8771972.html)

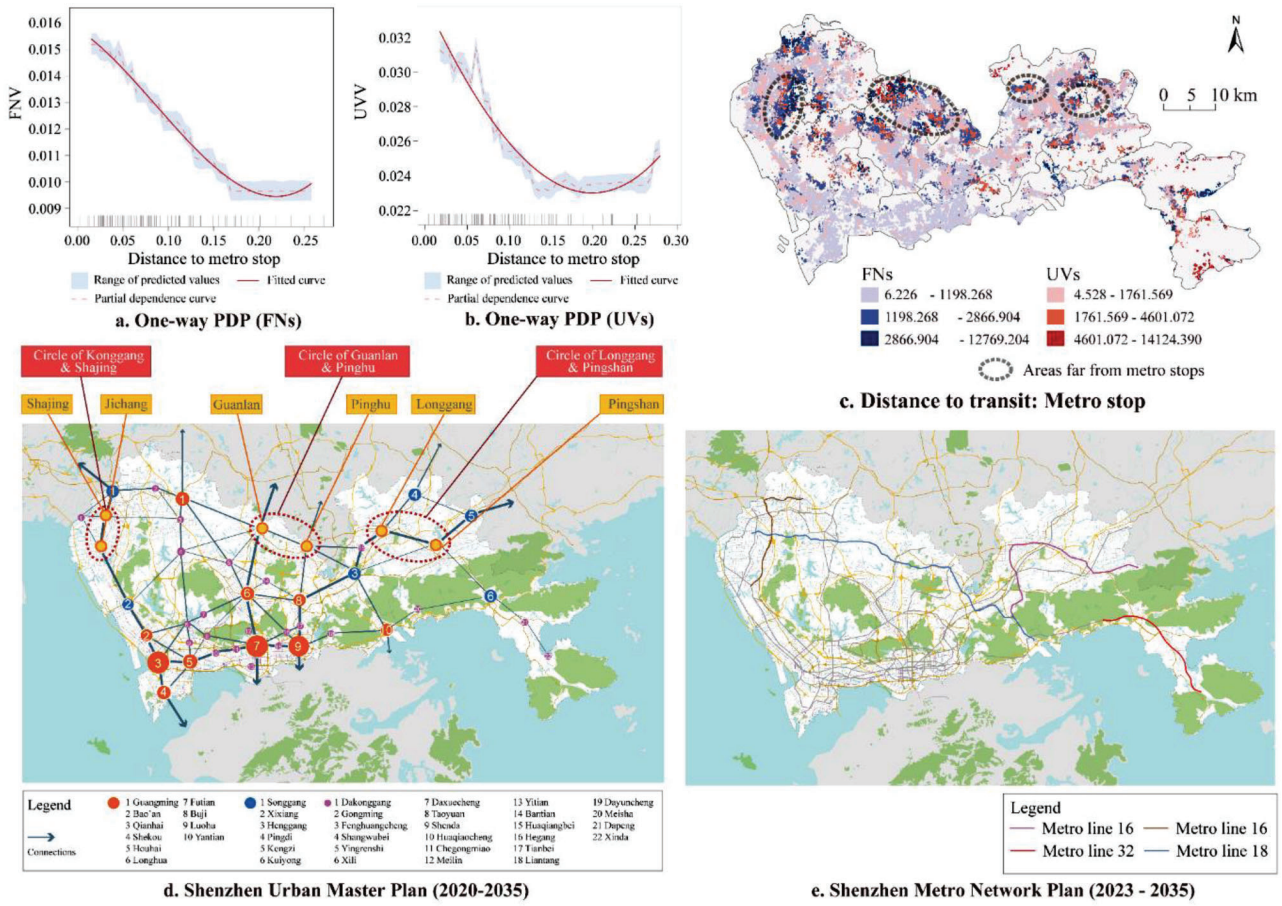

Fig. 10. Consistency verification of research findings with Shenzhen master plan and Shenzhen Metro Network Plan.

obtained for FNs. First, greenness contributes negatively to UVV. Fig. 9d.7 shows that a higher street segment length and lower greenness lead to higher UVV. Previous studies have emphasized that a lack of residential green spaces is detrimental to physical and mental health and neighborhood activities (Shanahan et al., 2016). However, the studies do not consider the type of high-density communities. The dense environment of UVs must provide multiple-functions (Van Oostrum, 2022), continuously squeezing green spaces. Moreover, the high-frequency commercial trade in the public spaces of UVs and high volume of commuter traffic inhibit the pursuit of green space. Second, higher building continuity (0.6 to 0.8) can generate more vitality (Fig. 9d.8). Excessive building continuity (> 0.8) might increase feelings of boredom and oppression (Zhang et al., 2021c)). Conversely, reduced building continuity (<0.2) leads to more exposure and reduces the sense of enclosure. Third, when openness is low (<0.2), high UVV emerges and is not influenced by street segment-length (Fig. 9d.9). The reduced openness in UVs helps boost vitality, explaining the reason for the dispersed highly positive correlation in the GTWR.

e. **FAR and FNV**

A one-way PDP illustrates the positive relationship between FAR and FNV (Fig. 9e.6). Fig. 9e.7 demonstrates that the higher the population density and FAR, the higher the FNV. Proximity to metro stops produces a similar correlation (Fig. 9e.9). Fig. 9e.8 presents an interesting phenomenon: when the distance to the bus stop is in a medium range (0.03 to 0.06) or farther (>0.08), there exists a positive correlation between FAR and FNV. We hypothesize that when the distance to the bus stop falls below 0.03 (distance less than 200 m), residents may prefer active travel modes. Conversely, FNs with distance coefficients exceeding 0.06 (distance above 2000 meters) typically lie in the remote suburbs, where residents tend to select more efficient modes of long-distance commuting. Moreover, the emergent polycentric urban structure of Shenzhen mitigates the dependence on public transit within FNs in remote suburbs (Yang et al., 2021b). Our study also indicates that a medium high BtA8000 (0.035 to 0.05) coupled with higher FAR, contributes to enhanced vitality (Fig. 9e.10).

The temporal differences displayed by GTWR manifest in the distribution of high values (Fig. 9e.1 to e.5). According to the natural-break method, high values at night are clustered in Futian, Bao'an, and Luohu, while medium-high value areas are distributed in the southern part of Luohu and Longhua and southwestern part of Longgang. Fig. 6 confirms the high correlation between night-time FNV and virtual vitality, while Fig. 9e.7 shows the positive correlation of FAR and population density with FNV. Based hereon, we used panel data from the population census to further cross-validate population density. Table 5 presents the population, area, and density of different districts. The population densities of Futian, Luohu, Longhua, Bao'an, and Longgang rank in the top five, which is consistent with observations, i.e., areas with high population density and high FAR represent greater FNV at night. Adequate population density is important to maintain the livability of a neighborhood (Li et al., 2022; Liu and Shi, 2022).

f. **FAR and UVV**

The relationship between FAR and UVV demonstrates a steady increase, reaching a peak of 0.04, higher than the 0.017 in FNs (Fig. 9f.6). The impact of population density on FAR and UVV exhibits similar trends in both UVs and FNs (Fig. 9f.7). Different from FNs, the distance to bus stops within UVs presents a unique pattern: the closer the distance to a bus stop and the higher the FAR, the greater the UVV (Fig. 9f.8). Additionally, a closer distance to metro stops generates a positive relationship between FAR and UVV (Fig. 9f.9). Incorporating the GTWR results (Fig. 9f.1 to f.5), we discover that the weak correlation between FAR and UVV across the entire temporal spectrum exists in the eastern (Longgang, Pingshan, and Dapeng) and western (Kungang and Shajing) suburbs. Our findings are consistent with those obtained by Hu et al. (2018a), indicating that urban public transportation facilitates weekend travel for residents of UVs. Concurrently, we identified that weekend travel among FN residents in the distant suburbs was not influenced by the availability of public transportation.

We compared the relationship between metro accessibility and NV, thus verifying the effectiveness of Shenzhen's master plan (Fig. 10d). One-way PDPs underscore that a greater distance to a metro stop hinders the emergence of NV. We found that these greater distances were primarily situated in the northern parts of Bao'an and Longhua, northeastern parts of Longgang, and the Pingshan District (Fig. 10c).

Consistent with the strategies emphasized in the Shenzhen Urban Rail Transit Network Planning (2016–2035) (Shenzhen Municipal Planning and Land & Resources Commission Marine Affairs Bureau, 2017) and Shenzhen Urban Master Plan (2020–2035) (Shenzhen Planning & Natural Resources, 2021), a "multi-center, networked, and clustered" approach has been advocated to enhance the guiding influence of rail transit on vitality and spatial development. The master plan underscores the necessity of shaping a clustered urban spatial structure through metro transit, designating Konggang and Shajing, Guanlan and Pinghu, and Longgang and Pingshan as the three main peripheral centers. They synergize with the radial structure of the urban center, aspiring to rectify the current imbalanced disposition of Shenzhen, where the west outweighs the east and the south surpasses the north. As evidenced in the latest plan, through the introduction of metro line 16 connecting Longgang with Pingshan, the proposed line 18 linking Guanlan and Pinghu, and line 26 enhancing connectivity between the airport and Shajing, the master plan utilizes metro transportation to interconnect and stimulate the development of urban periphery. It offers an insightful solution to the urban issues identified in this research.

4.3.2. Impact of objective eye-level features on NV

g. **Greenness in FNs**

A one-way PDP reveals a non-linear relationship between greenness and FNV, first decreasing then sharply increasing, suggesting a complex impact of greenness on FNV (Fig. 11g.1). The decrease in openness enhances the positive correlation between greenness and FNV. This is because an enclosed environment abundant with vegetation can increase residents' sense of security. Noteworthily, the peak values of FNV are realized when both greenness (>0.5) and openness (>0.57) are high (Fig. 11g.2). We infer that these conditions typically correspond to the public green spaces within FNs, which are likely to stimulate increased social interaction and crowd-based activities.

h. **Greenness in UVs**

An one-way PDP demonstrates a negative correlation between greenness and UVV, with UVV values ranging from 0.026 to 0.030, suggesting that greenness can stimulate UVV; however, an excessive proportion of greenness might hinder vitality production (Fig. 11h.6). A two-way PDP shows that a decrease in openness could promote a positive relationship between greenness and UVV, which is largely due to the distinctive high-density built environment in UVs (Fig. 11h.7). Noteworthily, the lower the probability of the presence of green space near UVs, the stronger the UVV, a finding that is consistent with existing research (Zhang et al., 2021d) (Fig. 11h.8). Streets and community green spaces expose residents to more options, as opposed to only urban green spaces. Furthermore, more mixed land-use patterns and increased walkability contribute to enhancing the relationship between green spaces and UVV (Fig. 11h.9 and h.10). The efficient and compact built environment in UVs allows residents to have more contacts with a greater variety of living service facilities within a shorter time, which is also among the goals of creating "15-minute living circles" (Zhang et al., 2022).

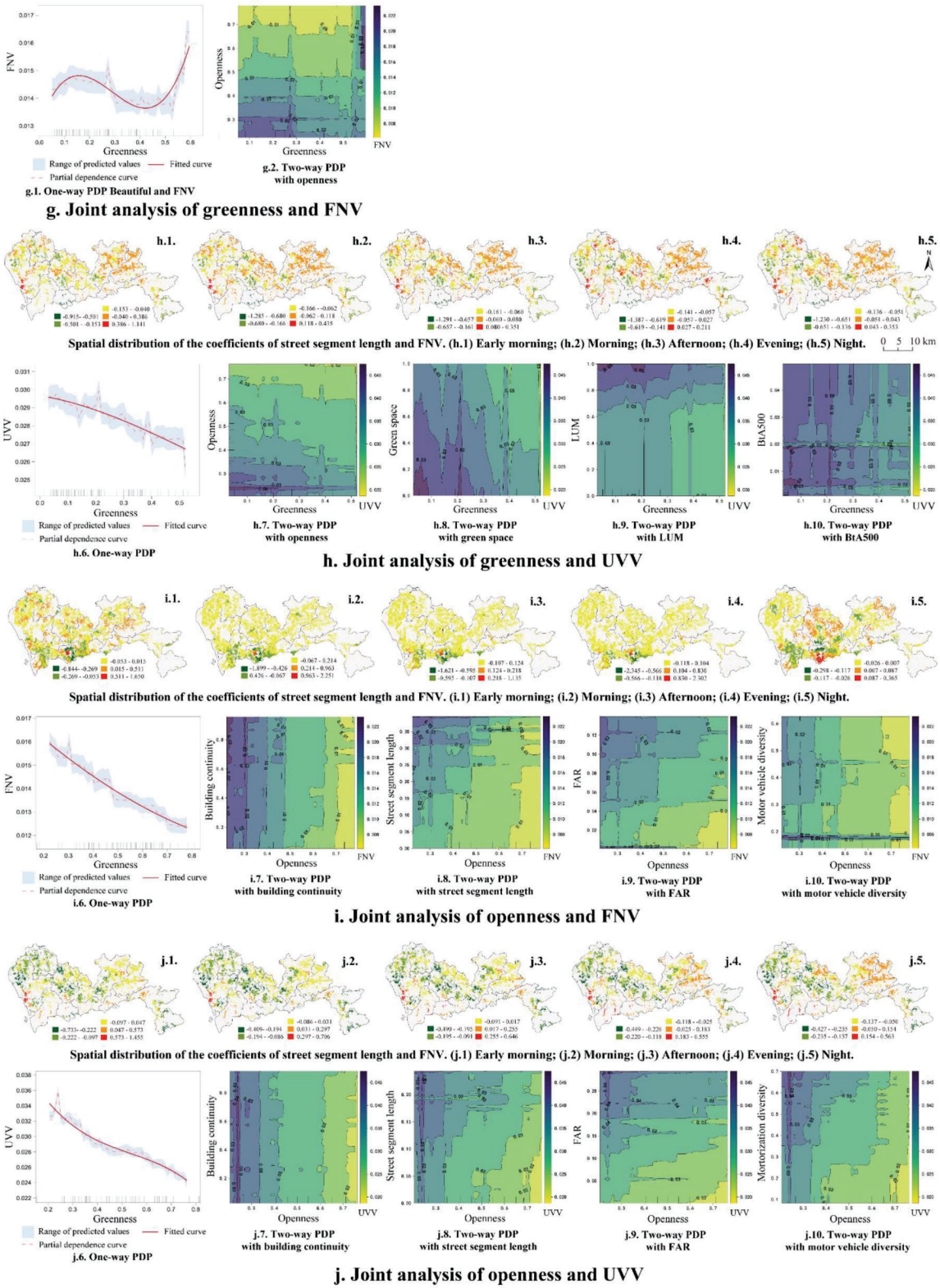

Fig. 11. Joint analysis of variable cluster II regarding FNV and UVV.

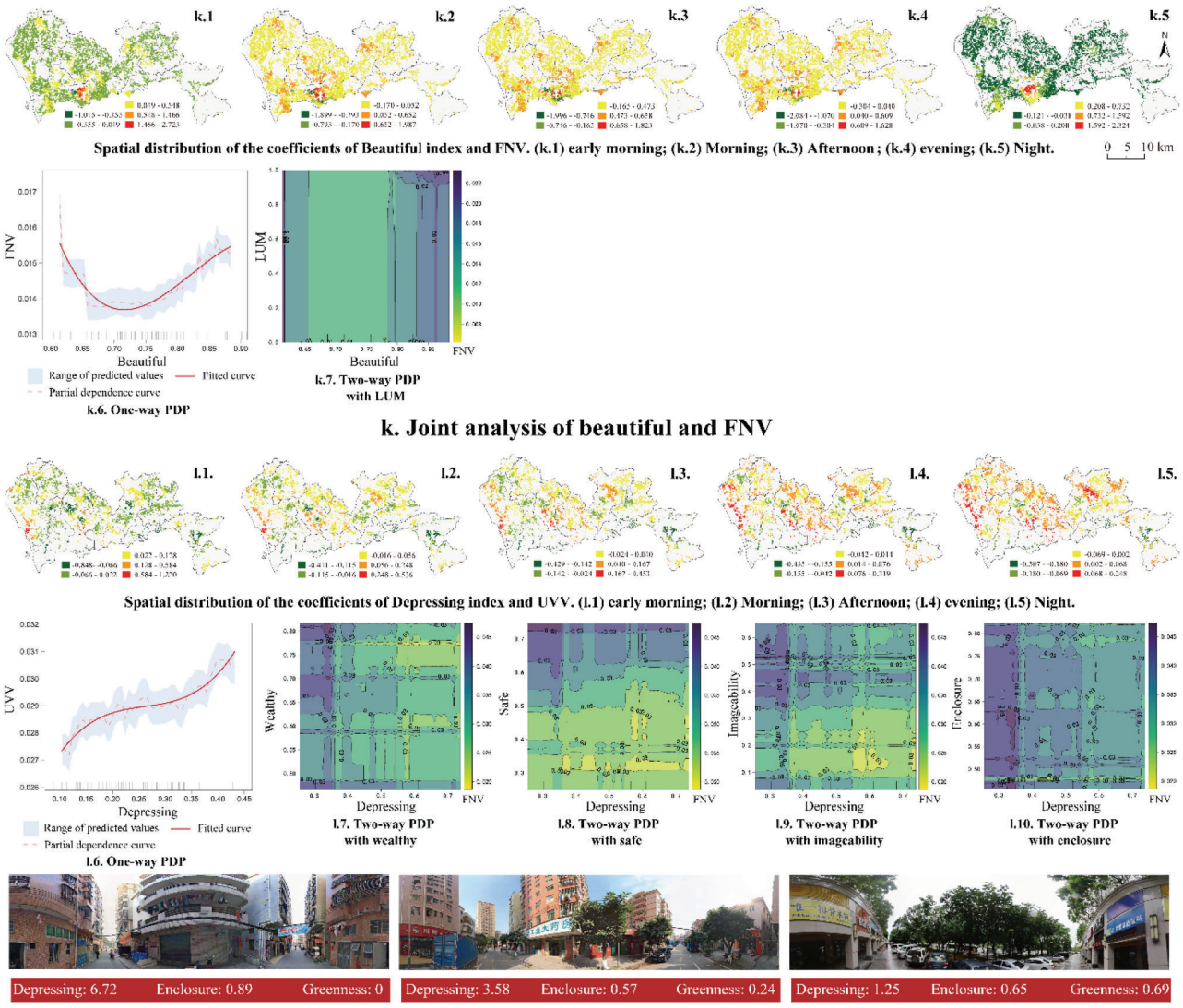

Fig. 12. Joint analysis of variable cluster III regarding FNV and UVV.

GTWR reveals a geographically uneven distribution of high and low values, and this distribution is unaffected by temporal changes (Fig. 11h.1 to h.5). Notably, in Bao'an's-UVs, the positive correlation between greenness and UVV is most pronounced, whereas the core areas exhibit a significant negative correlation. Further exploration of this phenomenon is expected.

i. Openness in FNs

Openness exhibits a negative relationship with FNV (Fig. 11i.6). An increase in building continuity can enhance the relationship between openness and FNV (Fig. 11i.7). A similar effect is discovered in the context of street segment length and FAR (Fig. 11i.8). The enhancement of street network density can promote commuting efficiency, while an increase in FAR can accommodate more residents (Fig. 11i.9). We found that low motor vehicle diversity (0.2) generated a threshold effect, where fewer types of motor vehicles led to increased FNV (Fig. 11i.10). It is plausible that this relationship stems from the extensive variety of motorized vehicles present in these areas. Our findings underscore that high-density urban neighborhoods should align with reduced motorization to foster vitality (Guerra et al., 2019; Yin and Zhang, 2021).

j. Openness in UVs

In UVs, openness reveals a negative correlation with UVV (Fig. 11j.6). Distinct from FNs, a higher diversity of motorized vehicles within UVs has been observed to intensify this negative correlation between openness and UVV. The increased presence of motor vehicles may compromise travel safety in FNs (Marquet and Miralles-Guasch, 2015; Yin and Zhang, 2021). However, a greater number of vehicles in UVs indicates busier commercial activities and commuting statuses, increasing the attractiveness and participation rate of the area (Guerra et al., 2019; Singh, 2016). GTWR shows that high-value areas are concentrated in Bao'an, with a few located in the Nanshan and Futian districts (Fig. 11j.1 to j.5). In the densely populated UVs, public spaces characterized by a high openness index can enhance community vitality at all times. Studies have shown that well-designed public open spaces in neighborhoods can encourage physical activity, contributing to the health of local residents's health. (Giles-Corti et al., 2005). However, the public spaces in UVs are currently being encroached upon. The fact that these public spaces are becoming a scarce resource necessitates more attention and protection (Van Oostrum, 2022).

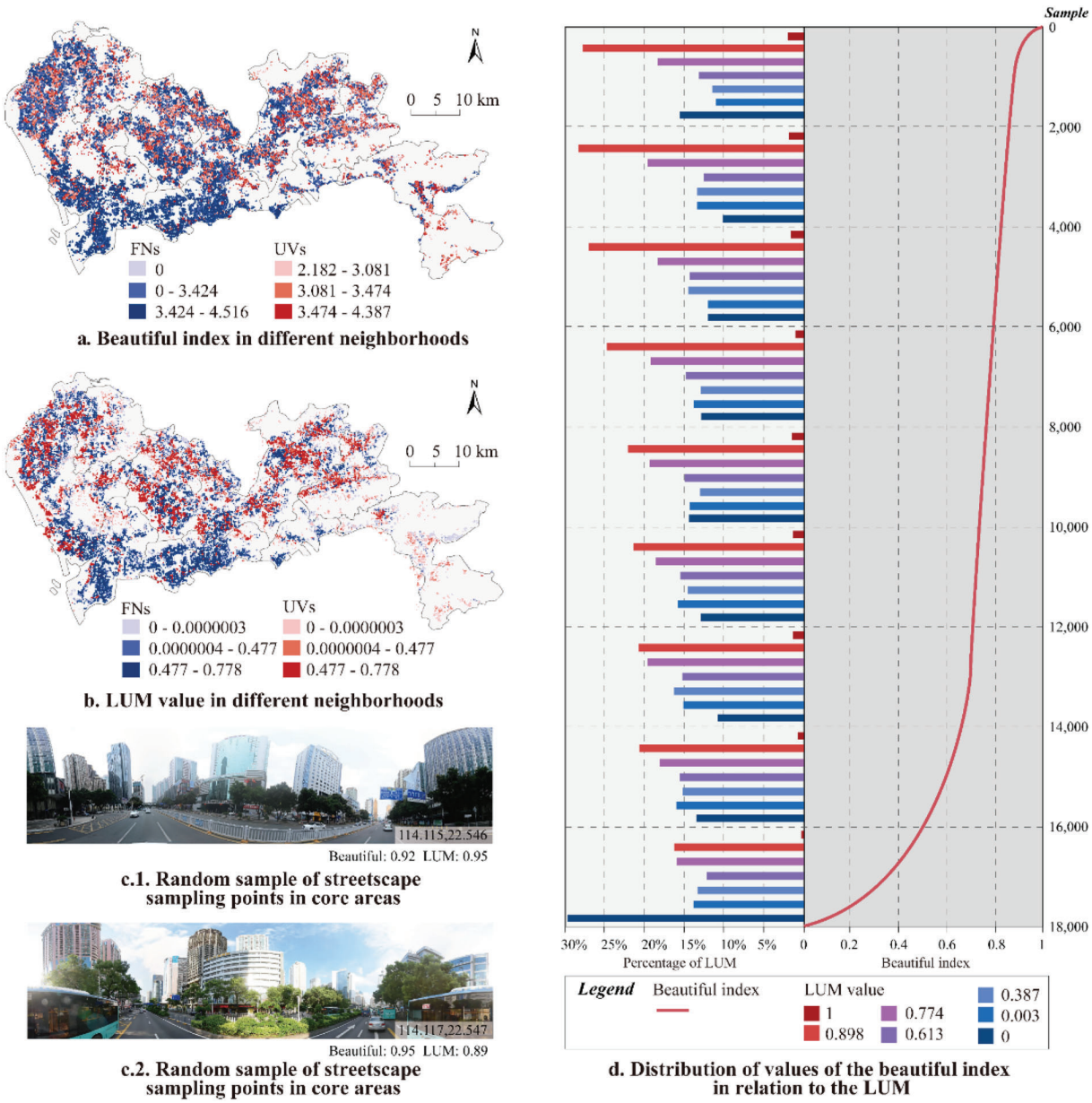

Fig. 13. Verification of the relationship between Beautiful Index and Land Use Mix (LUM).

4.3.3. Impact of subjective eye-level perceptions on NV

k. Beautiful in FNs

Fig. 12k.6 shows a nonlinear relationship between the "beautiful" index and FNV. This conclusion challenges existing findings that "beautiful" has a negative impact on vitality (Wu et al., 2023). Scholars have explained that beautiful places may have monotonous urban functions, inhibiting the occurrence of the street boundary effect, thus reducing social interactions. To further verify this hypothesis, we first compared the geographical distribution of "beautiful" and LUM (Fig. 13a and b). The visualization map shows that the high-value areas of "beautiful" are scattered across different districts, especially in the core areas. The distribution of LUM is similar, but the low values in Longgang, Longhua, and Bao'an are more frequent than those for "beautiful". Consequently, we analyzed the frequency distribution of LUM values by sorting "beautiful" from high to low (Fig. 13d). We found that as the 'beautiful' index decreased, the frequency of high LUM values did not decrease but showed a similar distribution. This indicates that the scores for "beautiful" are not related to the highs and lows of LUM. Fig. 13c displays the SVIs of areas with the highest LUM (defining the first category in the natural break method as the highest), and it was observed that the "beautiful" index was also high. Therefore, the assumption that beautiful urban spaces have a single function is unfounded (Wu et al., 2023).

GTWR shows that the correlation coefficients of "beautiful" in the morning, afternoon, and evening are generally higher than those in the early morning and night (Fig. 12k.1 to k.5). This is consistent with common sense, as residents identifying whether a space is beautiful first requires regular travel times and sufficient lighting conditions. During the early morning and night periods, GTWR indicates a large area of negative values, which might be one of the reasons explaining the nonlinear relationship in which 'beautiful' and FNV show a negative correlation.

l. Depressing in UVs

Jia et al. (2022) found that a higher "depressing" index negatively impacted house prices, and they explained that the "depressing" index was due to the increase in natural landscapes and trees. We found that as the "depressing" index increased, it became more detrimental to vitality (Fig. 12l.6). Subsequently, by randomly sampling SVIs with different depressing indices, we found that depressing spaces often exhibited higher "enclosure" and lower "greenness" (Fig. 12l.11). In other words, more enclosed spaces and less contact with greenery are the reasons for the depression (Helbich et al., 2019; Rui, 2023b). We further explored the joint effects of other subjective spatial perceptions and "depressing" on UVV. Two-way PDPs show that environments that appear wealthier and safer can enhance UVV with lower depressing levels (Fig. 12l.7 and l.8). Higher "imageability" and more openness can have the same effect (Fig. 12l.9 and l.10). GTWR shows that in Nanshan, southern Longhua, and northeastern Longgang, the "depressing" index and UVV are continuously increasing and expanding over time, peaking at night (Fig. 12l.1 to l.5). Wen et al. (2017) explained this phenomenon, i.e., the floating population in UVs has depressing emotions due to long working hours, social status, and economic reasons.

5. Discussion

5.1. New insights into NV

By quantifying the vitality of different neighborhoods across various time intervals, we identified the heterogeneous distribution of residents' online and offline activities both geographically and temporally, and we uncovered disparities inherent in urban planning, thereby facilitating the development of targeted planning solutions. We challenged the negative relationship between road density and vitality, as well as the positive correlation between greenery and vitality, proposed in our second hypothesis and in existing studies. Li et al. (2022) used the entire city of Wuhan and found an inverse relationship between road density and vitality. However, our investigation unveiled a nonlinear relationship between road density and vitality within residential areas, characterized by a positive association in FNs, and an initial decline followed by an upturn in UVs. While greenness generally promotes FNV, its role is strikingly opposite in UVs. The contribution of green spaces to residents' health and vitality is not applicable to high-density UVs (Shanahan et al., 2016).

The collaborative effects of multimodalities further provide evidence to both confirm and refute the relationship between public transportation efficiency (especially metro) and NV. We first demonstrated the crucial role of subways in downtown residential areas. A PDP revealed a negative correlation between metro stop proximity and the FNV and UVV. Areas far from metro stops were identified. Our research on suburban vitality and metro accessibility validates the effectiveness of developing peripheral urban centers as stated in Shenzhen Urban Master Plan (2020–2035) (Shenzhen Planning and Natural Resources Bureau, 2021) and the Shenzhen Urban Rail Transit Network Planning (2016–2035) (Shenzhen Municipal Planning and Land & Resources Commission Marine Affairs Bureau, 2017). However, the collaborative analysis refuted the contribution of transportation in far suburbs as the high population density in UV seemed to overcome the dependency on proximity to city centers. This finding substantiates the transformation of UVs into "micro special economic zones" anchored in e-commerce (Tang and Zhu, 2020), thereby stimulating intra-regional circulation and championing a polycentric urban growth pattern.

5.2. Implications for shaping vibrant neighborhoods

For all neighborhoods, we found that increasing the density of public transportation and reducing the distance of stops to different neighborhoods could enhance vitality. Our study demonstrates that Shenzhen's prospective metro planning harbors the capability to catalyze the development of three significant peripheral urban hubs, thereby enhancing the connectivity of relatively later-developing areas such as Longgang and Pingshan.

For FNs, it may be worth considering the reduction of both the intensity and variety of motor vehicles for safety reasons. Given the lower building densities in FNs, more green spaces could potentially enhance aesthetic appeal and stimulate residents' activities. For UVs, the first consideration is to reconstruct street space for multiple functionalities. Clearly delineating road rights can enhance commuting efficiency for motor vehicles while also ensuring the safety of active travel. Efficiency in narrow streets could be improved by implementing one-way systems. Additionally, more street greenery can serve beautification and buffer functions (Li et al., 2022; Xia et al., 2020). Furthermore, it is critical that UVs maintain their diverse and highly accessible public facilities. Such an approach extends services into the surrounding urban districts while facilitating the goal of constructing "15-minute living circles" (Zhang et al., 2022).

5.3. Eye-level spatial perceptions for bottom-up neighborhood planning

The aforementioned research outcomes, stemming from the dimension of the physical environment, provide planning insights for shaping community vitality. In the process of testing the third research hypothesis, we delved further into neighborhood design strategies from an eye-level perceptual perspective, advocating a bottom-up approach. These resident-centric strategies underscore the pivotal role of eye-level spatial measurement in augmenting traditional physical environment research.

We selected streetscape samples in FNs and UVs in central and suburban areas, based on the eye-level perceptual values to provide

Fig. 14. Subjective spatial perceptual scores and neighborhood vitality values in FNs and UVs.

resident-oriented planning recommendations (Fig. 14). For FNs, physical barriers on roads, such as railings or greenbelts, can be implemented. In suburban areas with ample street space, greenbelts could serve as effective separators, while in more dense contexts, railings could be considered. Moreover, existing research has demonstrated that the presence of diverse urban functions (stores, snack bars, etc.) along the streets can significantly bolster NV (Chen et al., 2023; Xia et al., 2020; Ye et al., 2018). Signage on building façades can increase the imageability of cities and alleviate boredom (Li et al., 2022; Lu et al., 2019; Wu et al., 2023). However, we found that the disorganized signage in suburban neighborhoods potentially contributed more to chaos than to aesthetics.

Unlike FNs, the compact spaces of UVs necessitate the accommodation of multifarious functions including commuting, automobile parking, and commerce (Van Oostrum, 2022). A multitude of vehicles indiscriminately parked within these limited spaces could exacerbate feelings of oppression and boredom, thereby compromising safety and aesthetic values. From a design perspective, reconfiguring residential parking spaces and considering the use of multi-story parking to increase space utilization can be useful. Interestingly, enhancing the richness of street facade colors appears to also boost aesthetic indices.

6. Conclusion

Our study contributes four theoretical insights: first, the redefinition of urban vitality; by constructing real and virtual vitality maps, this study redefines the concept of residential vitality, expanding the understanding of its interaction with virtual and physical spaces. Second, the proposition and verification of theoretical assumptions; this research posited three hypotheses concerning the research questions and validated them. Notably, the third theoretical assumption highlights that residential vitality is influenced not only by the physical environment but also by residents' spatial perception, thus establishing urban vitality as a multi-dimensional construct that requires analysis from multiple dimensions. Third, multi-model collaboration offers a comprehensive explanation of vitality: This study formulates a more comprehensive and refined theoretical model of NV. By utilizing collaborative interpretation, it unveils complex urban phenomena that a single theoretical framework may fail to capture, providing a new theoretical pathway for understanding the multifaceted nature of vitality. Fourth, the integration of empirical validation and theoretical application: through joint analysis, this study validates the rationality of the Shenzhen Urban Rail Transit Network Planning (2016–2035) (Shenzhen Municipal Planning and Land & Resources Commission Marine Affairs Bureau, 2017), highlighting the tight linkage between theory and practical application. Concurrently, through an examination of the "beautiful" index and LUM, this research refutes the assumption that "beautiful spaces are surrounded by single function," (Wu et al., 2023), further emphasizing the significant role of empirical research in advancing theoretical development.

We emphasize that a robust public transportation system can enhance the vitality of all neighborhoods. Regarding FNs, diminishing the heterogeneity of motorized vehicles can precipitate a safer environment, while an increase in green spaces and well-organized street signage can enhance visual aesthetics. For UVs, a clear right-of-way complemented with street trees can improve traffic efficiency and beautify the street environment. The preservation of diverse public facilities can expedite the realization of "15-minute living circles".

This study has some limitations. First, the targeted residential planning recommendations derived from a neighbourhood-centric research focus are not universally applicable to other urban functional zones. Future research could contemplate extending these recommendations to diverse urban functional areas, such as commercial, industrial, or mixed-use zones, to test the generalizability of these propositions. Second, the use of hexagonal grids with a side length of 200 meters has some discrepancy with the real morphological features of neighborhoods. Subsequent studies might explore the utilization of more precise morphologies of communities or other urban functions, or consider more sophisticated spatial analysis techniques, although this approach has its own drawbacks, namely the inability to control the size of the study units which may lead to biased outcomes for count-type variables. Third, the reasons for the observed non-linearity, specifically the negative correlation between the beautiful index and vitality, require further investigation. Future research could delve into potential moderating or mediating variables, and how "beauty" interacted with spatial vitality across varying cultural and socio-economic contexts.

CRediT authorship contribution statement

Jin Rui: Conceptualization, Data curation, Formal analysis, Investigation, Methodology, Project administration, Resources, Software, Supervision, Validation, Visualization, Writing – original draft, Writing – review & editing. **Xiang Li:** Methodology, Software, Visualization, Writing – original draft, Writing – review & editing.

Declaration of Competing Interest

The authors declare that they have no known competing financial interests or personal relationships that could have appeared to influence the work reported in this paper.

Data availability

Data will be made available on request.

Acknowledgment

We would like to extend our heartfelt gratitude to Ye Yanning, Xiang Qiuya, Chen yi, and other participants for their efforts in scoring the street view images.

Appendix

Entropy method

The Entropy Method, developed based on information entropy theory, is a multicriteria decision analysis technique extensively applied in evaluation and decision-making processes, especially when multiple variables or criteria must be considered concurrently. Information entropy, initially introduced by Shannon (1948), serves as a quantitative measure to gauge the uncertainty or complexity of information. In the Entropy Method, the weights of various evaluation criteria are determined by the amount of valid information they contain, meaning the more substantial the information, the higher the weight.

Distinct from other methodologies, the Entropy Method operates independently of decision-makers' subjective input, thereby significantly minimizing errors and biases that subjective elements might introduce, a contrast to methods like the Analytic Hierarchy Process (AHP) and Technique for Order of Preference by Similarity to Ideal Solution (TOPSIS), which involve subjective interventions. Moreover, the outcomes derived from the Entropy Method are not only highly consistent and reproducible but are also unaffected by changes in decision-makers.

Notably, the Entropy Method proves particularly potent when handling datasets with multiple variables and a large sample size. It can precisely dissect the influence of each variable on the overall data distribution, an aspect somewhat more reliable than Principal Component Analysis (PCA), which might lose some original data information during the dimensionality reduction process.

Global Moran's I

The global Moran's I examines spatial correlation patterns across the study area (Moran, 1950).

$$\text{Moran}'s\, I = \frac{\sum_{j=1}^{n}\sum_{j-1}^{n} w_{ij}(x_i - \overline{x})(x_i - \overline{x})}{S^2 \sum_{i=1}^{n}\sum_{j-1}^{n} w_{ij}} \tag{10}$$

where x_i and x_j represents the i and j values of the variable x on each unit, n is the total number of settlements, w_{ij} refers to spatial weight matrix, $\overline{x}$ represents the mean of spatial unit attributes.

Local Moran's I, referred to as Local Indicator of Spatial Association (LISA), is utilized to assess the statistical significance of spatial differences.

$$\text{LISA} = \frac{(X_i - X^-)}{S_X^2} \sum_{i=1}^{n} \left[w_{ij}(\mathrm{X}_i - \mathrm{X}^-) \right] \tag{11}$$

A positive LISA means a high value surrounded by a high value or a low value surrounded by a low value, namely, H-H or L-L. A negative LISA means that a low value is surrounded by a high value or a high value is surrounded by a low value, namely, H-L or L-H.

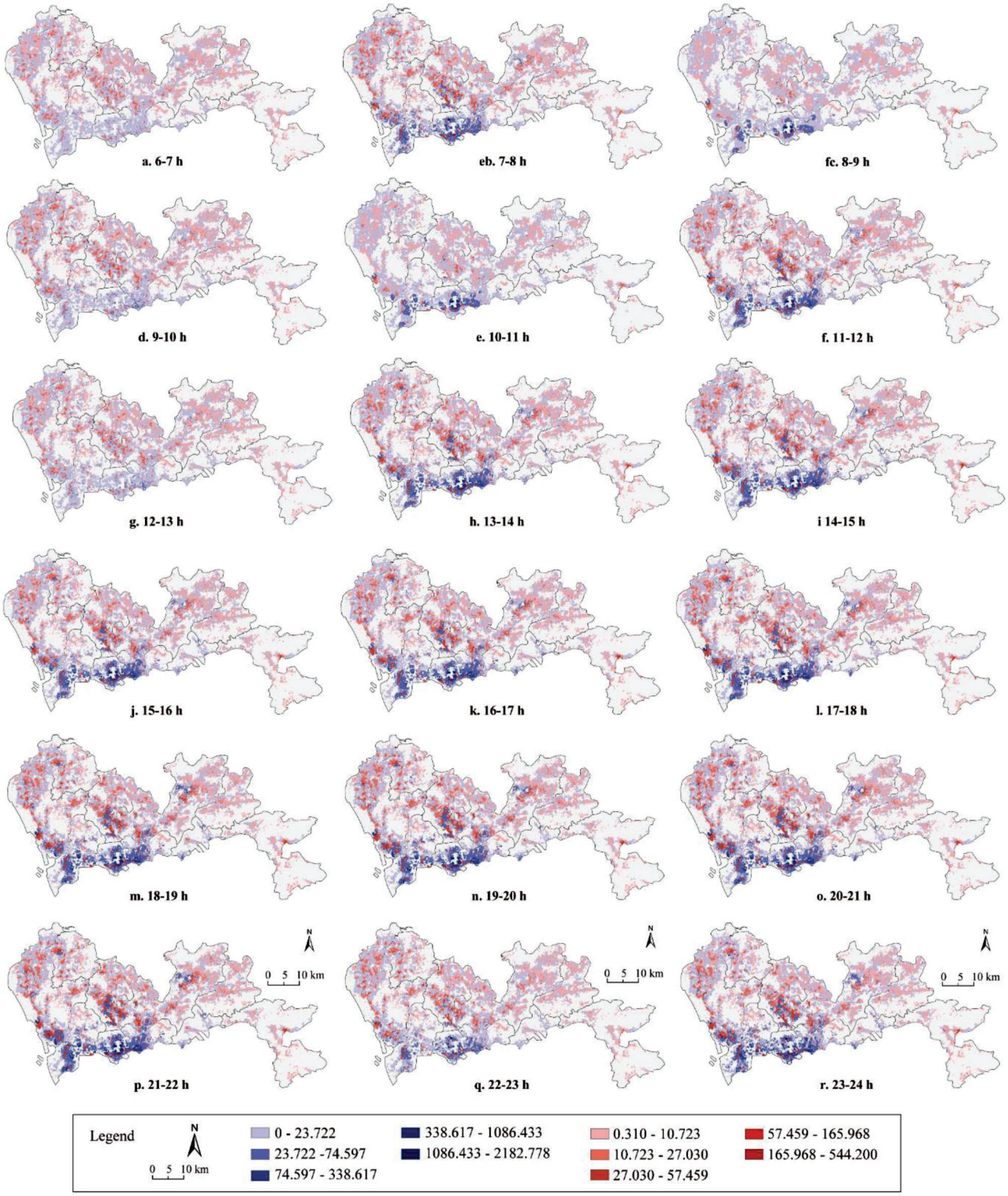

Fig. A1. The spatial distributions of FNV and UVV in Shenzhen.

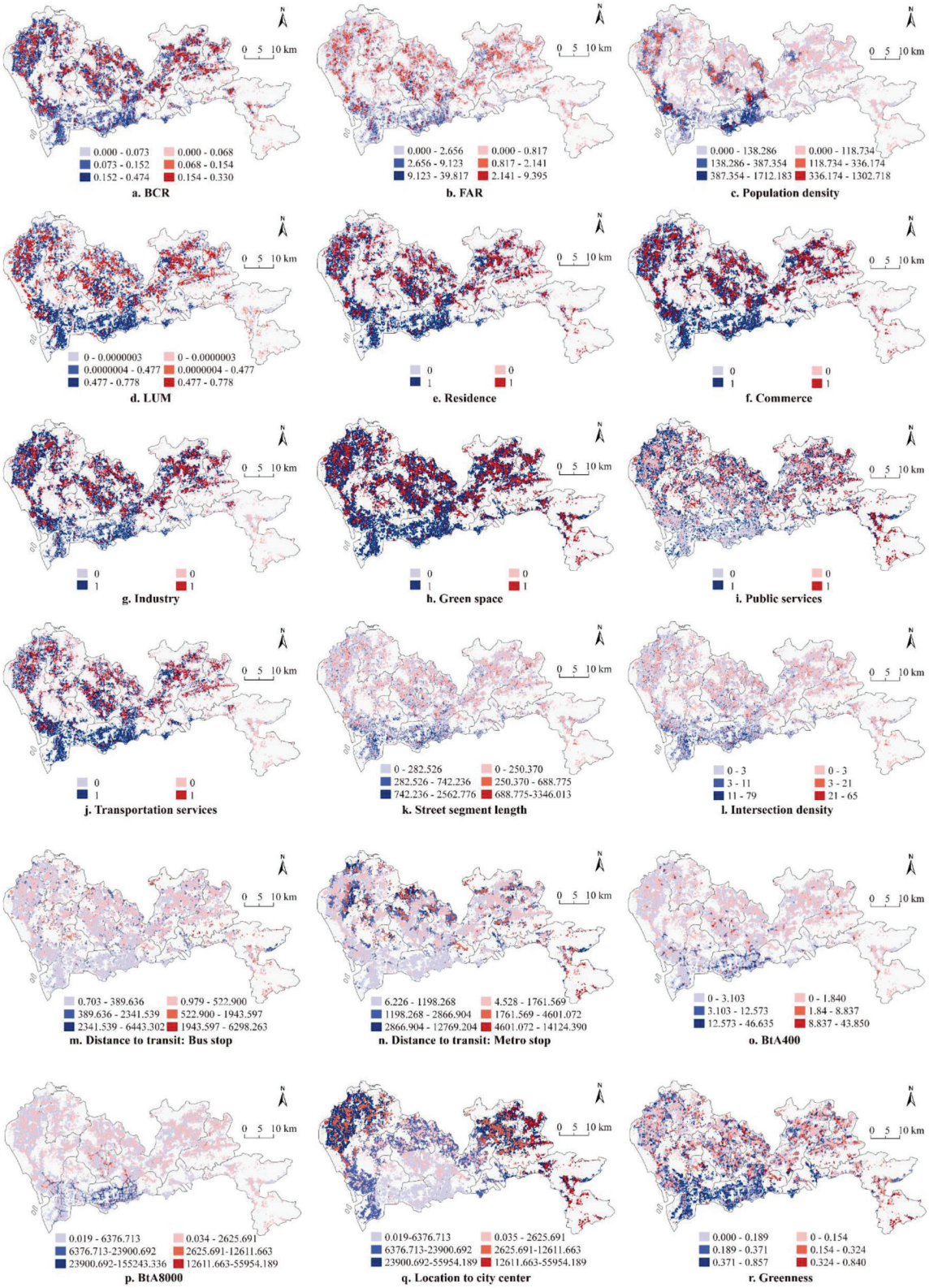

Fig. A2. The spatial distribution of values of all variables in the study area.

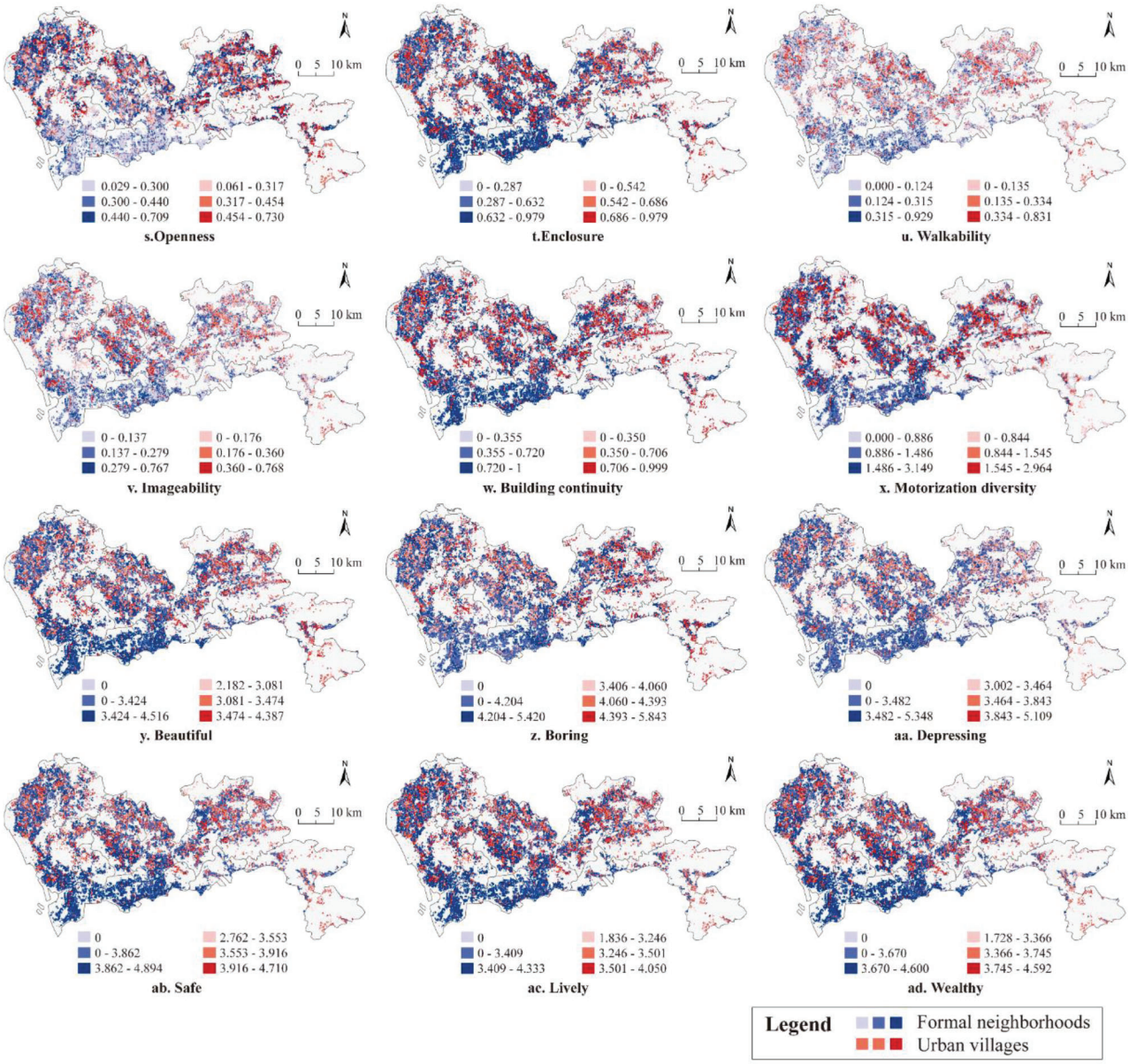

Fig. A2. (*continued*).

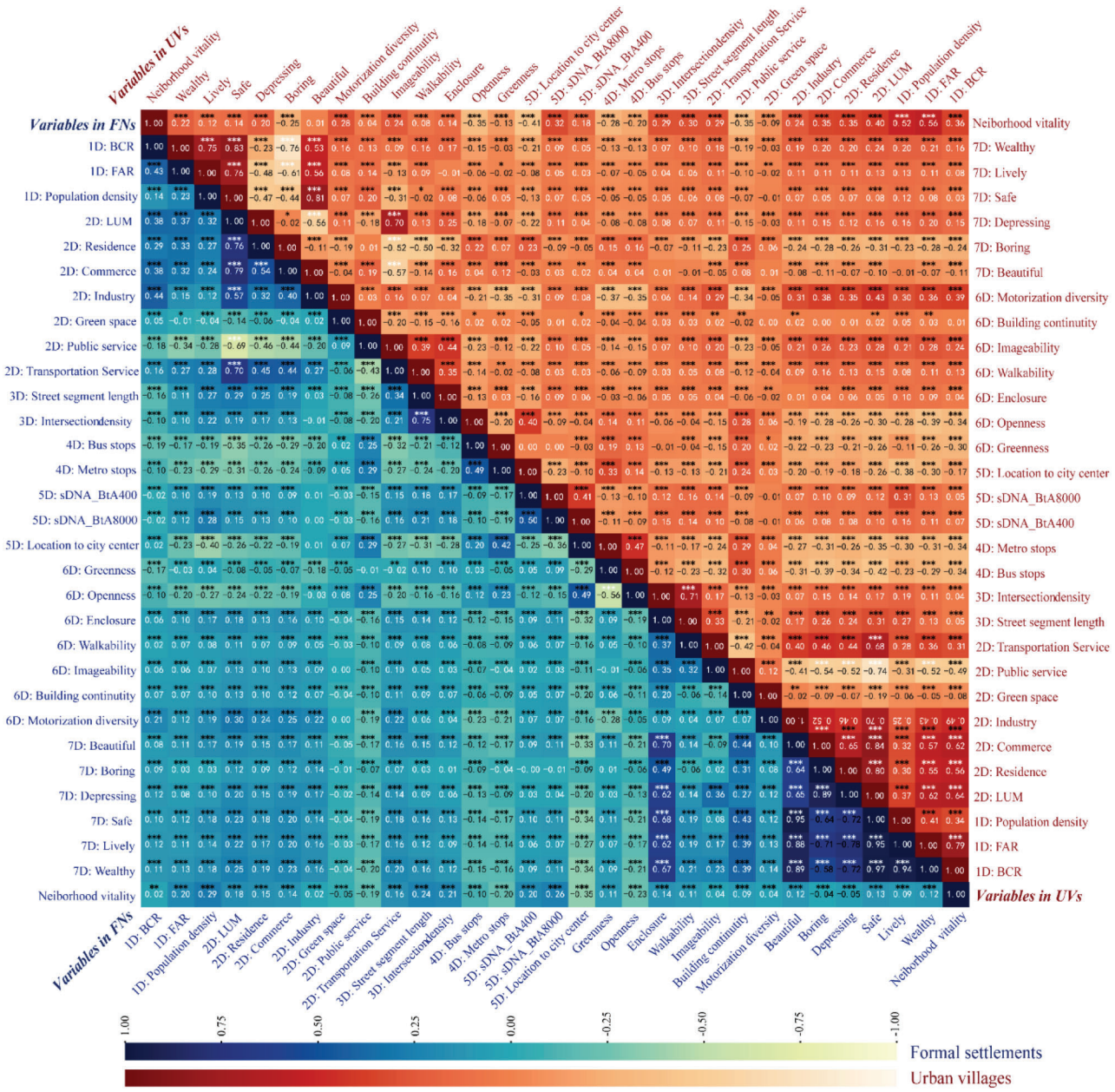

Fig. A3. Person correlations of all variables and neighborhood vitality in formal neighborhoods (blue) and urban villages (red). ***: $p < 0.001$, **: $p < 0.01$, *: $p < 0.05$.

Table A1
Data and sources.

Data	Sources	Access date
Baidu heat map	Baidu (https://lbsyun.baidu.com/)	April 29, 2023
Weibo check-in	Sina Weibo (https://m.weibo.cn/)	April 28, 2023
POI data	Baidu Map (https://lbsyun.baidu.com/)	April 25, 2023
NDVI	NASA's Earth Observing System Data and Information System Reverb (http://reverb.echo.nasa.gov/)	April 25, 2023
Urban administration, street and building footprint	OpenStreetMap (https://www.openstreetmap.org)	April 25, 2023
Street view image	Baidu map (https://lbsyun.baidu.com)	Mai 1, 2023
Population data	WorldPop (https://www.worldpop.org/)	April 25, 2023

Table A2
Descriptive statistics of dependent and independent variables.

Clusters	Variables	Min	Max	Mean	S.D.
Dependent variables	Real vitality	0	49.303	6.733	4.45
	Virtual vitality	0	1066.793	6.573	24.174
	Neighborhood vitality	0	1081.521	13.307	24.892
	FNV	0	1081.521	15.271	29.857
	FNV in the early morning	0.41	141.947	6.214	5.26
	FNV in the morning	0.479	308.907	9.656	9.433
	FNV in the afternoon	0.379	326.397	10.005	10.34
	FNV in the evening	0.31	464.305	12.223	13.89
	FNV at night	0.317	380.587	10.095	11.205
	UVV	0	320.774	9.675	9.836
	UVVV in the early morning	0	430.533	8.463	12.814
	UVV in the morning	0	1082.017	15.27	9.152
	UVV in the afternoon	0	1147.811	16.316	9.016
	UVV in the evening	0	1741.992	19.772	10.092
	UVV at night	0	1521.302	15.598	8.048
1D: Density	BCR	0	0.474	0.103	0.069
	FAR	0	39.817	1.448	2.017
	Population density	0	1712.183	107.694	121.811
2D: Diversity	LUM	0	0.778	0.394	0.283
	Residence	0	1	0.545	0.498
	Commerce	0	1	0.651	0.477
	Industry	0	1	0.586	0.493
	Green space	0	1	0.952	0.214
	Public service	0	1	0.488	0.5
	Transportation services	0	1	0.476	0.499
3D: Design	Street segment length	0	3346.013	337.072	317.494
	Intersection density	0	79	1.726	3.176
4D: Distance to transit	Bus stop	0.702	6443.302	254.763	326.875
	Metro stop	4.528	14124.39	1298.398	1215.537
5D: Destination accessibility	BtA400	0	46.635	0.9	2.443
	BtA8000	0.02	155243.336	1236.807	4265.359
	Location to city center	443.752	56523.736	22890.842	1099.831
Objective spatial features	Greenness	0	0.857	0.219	0.14
	Openness	0.029	0.73	0.386	0.116
	Enclosure	0	0.979	0.641	0.129
	Walkability	0	0.929	0.146	0.141
	Imageability	0	0.768	0.194	0.128
	Building continuity	0	1	0.667	0.279
	Motor vehicle diversity	0	3.149	1.299	0.48
Subjective spatial perceptions	Beautiful	0	4.516	3.324	0.513
	Boring	0	5.843	4.136	0.543
	Depressing	0	5.348	3.396	0.431
	Safe	0	4.894	3.773	0.537
	Lively	0	4.333	3.397	0.439
	Wealthy	0	4.6	3.618	0.527

Table A3
POI classification based on the Baidu platform.

Integration Clusters	Counts	POI classifications	Secondary classifications
Residence	30,499	Accommodation services	Communities, apartments, villas, dormitories etc.
Commerce	133,954	Business, commercial, entertainment, and other facilities	Shopping centers, restaurants, hotels, cinemas, banks etc.
Industry	90,755	Factories and industrial buildings	Companies, factories, science and technology parks, industrial parks, etc.
Public services	66,218	Land for cultural, educational, medical treatment and health, social welfare activities.	Education and culture services, health care services, sport and leisure services, government agencies, public facilities, etc.
Green space	2,637	Public places such as parks, green spaces, and squares.	Scenic spots, zoos, botanical gardens, parks, squares, etc.
Transportation services	47,081	All the roads, facilities, and junctions.	Parking lots, transport facility services, car and motorcycle services or repairs, etc. (Bus stations, metro stations and street intersections are excluded.)

Table A4
Accuracy of subjective spatial perception prediction models.

	Beautiful	Boring	Depressing	Safety	Lively	Wealthy	Mean
Mean squared error	0.62	0.64	0.58	0.73	0.64	0.63	0.64
Mean absolute error	0.63	0.63	0.61	0.67	0.64	0.64	0.64
R^2_score	0.32	0.16	0.21	0.24	0.20	0.28	0.24
Max error	2.63	2.47	2.20	2.79	2.49	2.31	2.48
Explained variance score	0.32	0.16	0.21	0.24	0.20	0.29	0.24

Table A5
The results of SWR models.

FNs								
Variables	Coefficient	St. Error	t	Probability	VIF	R^2	Adj. R^2	F
Intercept	30.487	0	13.743	0.000***	-	0.192	0.192	F=237.24, P=0.000***
BCR	-11.075	3.84	-2.884	0.004***	1.601			
FAR	1.187	0.1	11.873	0.000***	1.399			
Population density	0.027	0.002	14.859	0.000***	1.348			
Commerce	1.15	0.497	2.315	0.021**	1.405			
Green space	-4.874	1.887	-2.582	0.010***	1.831			
Street segment length	0.006	0.001	5.965	0.000***	2.588			
Intersection density	0.334	0.09	3.714	0.000***	2.317			
Bus stop	0.002	0.001	2.273	0.023**	1.431			
Metro stop	-0.001	0	-3.238	0.001***	1.582			
BtA400	0.464	0.083	5.606	0.000***	1.351			
BtA8000	0.001	0	12.658	0.000***	1.471			
Location to city center	0.00001	0	-17.527	0.000***	1.95			
Greenness	-4.874	1.887	-2.582	0.010***	1.831			
Openness	-17.466	2.435	-7.174	0.000***	1.999			
Walkability	11.11	1.529	7.268	0.000***	1.091			
Building continuity	2.514	0.826	3.045	0.002***	1.274			
Motor vehicle diversity	-2.84	0.503	-5.647	0.000***	1.276			
Beautiful	2.255	0.767	2.94	0.003***	5.063			
Lively	-4.027	0.846	-4.759	0.000***	4.894			
UVs								
Intercept	-6.492	2.217	-2.928	0.003***	-	0.511	0.51	F=561.762, P=0.000***
BCR	-24.395	1.715	-14.225	0.000***	3.335			
FAR	4.855	0.133	36.52	0.000***	3.157			
Population density	0.02	0.001	23.476	0.000***	1.505			
Residence	0.909	0.186	4.887	0.000***	1.728			
Industry	-0.558	0.172	-3.252	0.001***	1.489			
Green space	-1.691	0.285	-5.932	0.000***	1.014			
Street segment length	0.002	0	4.811	0.000***	2.305			
Intersection density	0.425	0.037	11.417	0.000***	2.066			
Bus stop	0.001	0	2.847	0.004***	1.44			
Metro stop	0.00003	0	-4.091	0.000***	1.498			
BtA8000	0.001	0	17.814	0.000***	1.146			
Location to city center	0.00001	0	-11.333	0.000***	1.537			
Greenness	-4.093	0.633	-6.471	0.000***	1.291			
Openness	-8.174	0.767	-10.65	0.000***	1.55			
Enclosure	2.149	0.711	3.024	0.003***	1.282			
Walkability	-1.077	0.512	-2.104	0.035**	1.173			
Depressing	-2.601	0.398	6.53	0.000***	1.672			
Safe	2.272	0.295	7.713	0.000***	1.529			

Table A6
Global Moran's I and z-score and p-value.

FNs				UVs		
Variables	Moran' I	Z-score	P value	Moran' I	Z-score	P value
BCR	0.128	104.365	<0.001	0.283	138.295	<0.001
FAR	0.201	163.990	<0.001	0.314	153.685	<0.001
Population density	0.698	570.194	<0.001	0.667	326.843	<0.001
LUM	-	-	-	-	-	-
Residence	-	-	-	0.207	101.457	<0.001
Commerce	0.136	111.342	<0.001	-	-	-
Industry				0.216	105.663	<0.001
Green space	0.033	26.976	<0.001	0.024	11.850	<0.001
Public service	-	-	-	-	-	-
Transportation services	-	-	-	-	-	-
Street segment length	0.289	235.732	<0.001	0.133	65.011	<0.001
Intersection density	0.267	218.529	<0.001	0.121	59.531	<0.001
Bus stop	0.207	169.844	<0.001	0.243	119.018	<0.001
Metro stop	0.604	493.021		0.564	276.204	<0.001
BtA400	0.313	255.448	<0.001	-	-	-
BtA8000	0.449	367.439	<0.001	0.171	84.847	<0.001
Location to city center	0.974	794.514	<0.001	0.835	408.651	<0.001
Greenness	0.410	335.025	<0.001	0.321	156.918	<0.001
Openness	0.524	427.288	<0.001	0.407	199.109	<0.001
Enclosure	-	-	-	0.166	81.293	<0.001
Walkability	0.136	110.798	<0.001	0.149	72.743	<0.001
Imageability	-	-	-	-	-	-
Building continuity	0.143	116.855	<0.001	-	-	-

(*continued on next page*)

Table A6 (*continued*)

FNs				UVs		
Motor vehicle diversity	0.280	228.825	<0.001	-	-	-
Beautiful	0.196	160.461	<0.001	-	-	-
Boring	-	-	-	-	-	-
Depressing	-	-	-	0.155	75.779	<0.001
Safe	-	-	-	0.125	61.182	<0.001
Lively	0.157	128.209	<0.001	-	-	-
Wealthy	-	-	-	-	-	-

Table A7
Comparison of different machine learning model performance.

	MSE		RMSE		MAE		MAPE	
FNs	Training set	Testing set	Training set	Testing set	Training set	Testing set	Training set	Testing set
Decision tree	0	0	0.011	0.005	0.007	0.004	43.192	51.84
Radom forest	0	0	0.012	0.005	0.006	0.004	38.154	49.845
K-nearest neighbors	0.001	0	0.026	0.006	0.008	0.004	36.823	48.31
Support vector machines	0.003	0.003	0.055	0.058	0.045	0.046	237.636	151.094
LightGBM	0.001	0	0.026	0.006	0.008	0.004	36.823	48.31
XGBoost	0	0	0.004	0.004	0.002	0.003	19.574	40.895
UVs	Train dataset	Test dataset	Train dataset	Test dataset	Train dataset	Test dataset	Train dataset	Test dataset
Decision tree	39.251	31.491	6.265	5.612	3.582	4.067	31.08	55.451
Radom forest	28.388	10.732	5.328	3.276	3.782	2.562	37.822	38.107
K-nearest neighbors	39.251	31.491	6.265	5.612	3.582	4.067	31.08	55.451
Support vector machine	35772	7629	189.14	87.35	163.517	69.487	109.717	112.526
LightGBM	13.42	9.634	3.663	3.104	2.513	2.302	27.198	37.146
XGBoost	1.629	9.776	1.276	3.127	0.9	2.293	11.915	37.895

References

Al_Sayed, K., Turner, A., Hillier, B., Iida, S., & Penn, A. (2014). Space syntax methodology: Bartlett school of architecture. *Londres: University*. https://doi.org/10.5354/0716-8772.2007.28222

Antoniadis, P., & Apostol, I. (2014). The Right (s) to the Hybrid City and the Role of DIY Networking. *The Journal of Community Informatics, 10*(3), 1–14.

Chen, T., & Guestrin, C. (2016). Xgboost: A scalable tree boosting system. In *Proceedings of the 22nd ACM sigkdd international conference on knowledge discovery and data mining* (pp. 785–794).

Chen, J., Tian, W., Xu, K., & Pellegrini, P. (2022). Testing small-scale vitality measurement based on 5D model assessment with multi-source data: A resettlement community case in Suzhou. *ISPRS International Journal of Geo Information, 11*(12), 626. https://doi.org/10.3390/ijgi11120626

Chen, Y., Yu, B., Shu, B., Yang, L., & Wang, R. (2023). Exploring the spatiotemporal patterns and correlates of urban vitality: Temporal and spatial heterogeneity. *Sustainable Cities and Society, 91*, Article 104440. https://doi.org/10.1016/j.scs.2023.104440

Chiaradia, A., Cooper, C., & Webster, C. (2012). *sDNA a software for spatial design network analysis, specifications*. Cardiff University.

China Academy of Urban Planning and Design. (2022). Commuting Monitoring Report for Major Cities in China. In M. o. H. a. U.-R. D. (Ed.), Urban Transportation Infrastructure Monitoring and Governance Laboratory. Retrieved from https://huiyan.baidu.com/reports/landing?id=123 (Accessed July 2023).

Cooper C.H., Chiaradia A.J., 2020, sDNA: 3-d spatial network analysis for GIS, CAD, Command Line & Python, SoftwareX 12:100525. 10.1016/j.softx.2020.100525.

Dong, L., Jiang, H., Li, W., Qiu, B., Wang, H., & Qiu, W. (2023). Assessing impacts of objective features and subjective perceptions of street environment on running amount: A case study of Boston. *Landscape and Urban Planning, 235*, Article 104756. https://doi.org/10.1016/j.landurbplan.2023.104756

Ewing, R., & Handy, S. (2009). Measuring the unmeasurable: Urban design qualities related to walkability. *Journal of Urban Design, 14*(1), 65–84. https://doi.org/10.1080/13574800802451155

Fan Z., Duan J., Lu Y., Zou W., Lan W., 2021, A geographical detector study on factors influencing urban park use in Nanjing, China, Urban Forestry & Urban Greening 59: 126996. 10.1016/j.ufug.2021.126996.

Forlano, L. (2013). Making waves: Urban technology and the co–production of place. *First Monday, 18*(11). https://doi.org/10.5210/fm.v18i11.4968

Giles-Corti, B., Broomhall, M. H., Knuiman, M., Collins, C., Douglas, K., Ng, K., Lange, A., & Donovan, R. J. (2005). Increasing walking: how important is distance to, attractiveness, and size of public open space? *American Journal of Preventive Medicine, 28*(2), 169–176.

Guerra, E., Dong, X., & Kondo, M. (2019). Do denser neighborhoods have safer streets? Population density and traffic safety in the philadelphia region. *Journal of Planning Education and Research*. https://doi.org/10.1177/0739456X19845043, 0739456X19845043.

Gupta, K., Kumar, P., Pathan, S. K., & Sharma, K. P. (2012). Urban Neighborhood Green Index–A measure of green spaces in urban areas. *Landscape and Urban Planning, 105*(3), 325–335. https://doi.org/10.1016/j.landurbplan.2012.01.003

Helbich, M., Yao, Y., Liu, Y., Zhang, J., Liu, P., & Wang, R. (2019). Using deep learning to examine street view green and blue spaces and their associations with geriatric depression in Beijing, China. *Environment International, 126*, 107–117.

Hu, H., Xu, J., Shen, Q., Shi, F., & Chen, Y. (2018a). Travel mode choices in small cities of China: A case study of Changting. *Transportation Research Part D Transport and Environment, 59*, 361–374. https://doi.org/10.1016/j.trd.2018.01.013

Hu, H., Xu, J., Shen, Q., Shi, F., & Chen, Y. (2018b). Travel mode choices in small cities of China: A case study of Changting. *Transportation research part D: transport and environment, 59*, 361–374.

Huang, B., Wu, B., & Barry, M. (2010). Geographically and temporally weighted regression for modeling spatio-temporal variation in house prices. *International Journal of Geographical Information Science, 24*(3), 383–401. https://doi.org/10.1080/13658810802672469

Huang, X., Jiang, P., Li, M., & Zhao, X. (2022). Applicable framework for evaluating urban vitality with multiple-source data: Empirical research of the pearl river delta urban agglomeration using BPNN. *Land, 11*(11), 1901. https://doi.org/10.3390/land11111901

Jacobs, A. B. (1993). *Great streets*. University of California Transportation Center.

Jia, J., Zhang, X., Huang, C., & Luan, H. (2022). Multiscale analysis of human social sensing of urban appearance and its effects on house price appreciation in Wuhan, China. *Sustainable Cities and Society, 81*, Article 103844. https://doi.org/10.1016/j.scs.2022.103844

Jiang Haiyan, S. T., Shijie, Li, & Zhiping, Deng (2023). Spatial pattern characteristics of urban virtual-real vitality in the digitization context: A case study of Guangzhou. *Tropical Geography, 43*(4), 695–706.

Kang, C., Fan, D., & Jiao, H. (2021). Validating activity, time, and space diversity as essential components of urban vitality. *Environment and Planning B: Urban Analytics and City Science, 48*(5), 1180–1197. https://doi.org/10.1177/2399808320919771

Kim, Y. L. (2018). Seoul's Wi-Fi hotspots: Wi-Fi access points as an indicator of urban vitality. *Computers, Environment and Urban Systems, 72*, 13–24.

Lai, G., Shang, Y., He, B., Zhao, G., & Yang, M. (2022). Revealing taxi interaction network of urban functional area units in shenzhen, China. *ISPRS International Journal of Geo Information, 11*(7), 377. https://doi.org/10.3390/ijgi11070377

Lan, F., Gong, X., Da, H., & Wen, H. (2020). How do population inflow and social infrastructure affect urban vitality? Evidence from 35 large-and medium-sized cities in China. *Cities, 100*, Article 102454. https://doi.org/10.1016/j.cities.2019.102454

Lee, S.h., & Kang, J. E. (2022). Impact of particulate matter and urban spatial characteristics on urban vitality using spatiotemporal big data. *Cities, 131*, Article 104030. https://doi.org/10.1016/j.cities.2019.102454

Li, X., Santi, P., Courtney, T. K., Verma, S. K., & Ratti, C. (2018). Investigating the association between streetscapes and human walking activities using Google Street

View and human trajectory data. *Transactions in GIS, 22*(4), 1029–1044. https://doi.org/10.1111/tgis.12472
Li, J., Li, J., Yuan, Y., & Li, G. (2019). Spatiotemporal distribution characteristics and mechanism analysis of urban population density: a case of Xi'an. *Cities, 86*, 62–70. https://doi.org/10.1016/j.cities.2018.12.008
Li, X., Li, Y., Jia, T., Zhou, L., & Hijazi, I. H. (2022). The six dimensions of built environment on urban vitality: fusion evidence from multi-source data. *Cities, 121*, Article 103482. https://doi.org/10.1016/j.cities.2021.103482
Liu, H., & Li, X. (2022). Understanding the driving factors for urban human settlement vitality at street level: A case study of Dalian. *Land*, (5), 646. https://doi.org/10.3390/land11050646
Liu, D., & Shi, Y. (2022). The influence mechanism of urban spatial structure on urban vitality based on geographic big data: A case study in downtown Shanghai. *Buildings, 12*(5), 569. https://doi.org/10.3390/buildings12050569
Long, Y., & Huang, C. (2019). The impact of urban design on economic vitality for Chinese cities. *Environment Planning B Urban Analytics and City Science, 46*(3), 406–422. https://doi.org/10.1177/2399808317715640
Lu, S., Shi, C., & Yang, X. (2019). Impacts of built environment on urban vitality: Regression analyses of Beijing and Chengdu, China. *International Journal of Environmental Research and Public Health, 16*(23), 4592. https://doi.org/10.3390/ijerph16234592
Lyu F., Zhang L., 2019, Using multi-source big data to understand the factors affecting urban park use in Wuhan, Urban Forestry & Urban Greening 43:126367. 10.1016/j.ufug.2019.126367.
Ma, X., Ma, C., Wu, C., Xi, Y., Yang, R., Peng, N., Zhang, C., & Ren, F. (2021). Measuring human perceptions of streetscapes to better inform urban renewal: A perspective of scene semantic parsing. *Cities, 110*, Article 103086. https://doi.org/10.1016/j.cities.2020.103086
Marquet, O., & Miralles-Guasch, C. (2015). Neighbourhood vitality and physical activity among the elderly: The role of walkable environments on active ageing in. *Social Science & Medicine, 135*, 24–30. https://doi.org/10.1016/j.socscimed.2015.04.016
McQuire, S. (2017). *Geomedia: Networked cities and the future of public space.* John Wiley & Sons.
Moran, P. A. (1950). Notes on continuous stochastic phenomena. *Biometrika, 37*(1/2), 17–23.
Oldenburg, R. (2001). *Celebrating the third place: Inspiring stories about the great good places at the heart of our communities.* Da Capo Press.
Ou, G., Zhou, M., Zeng, Z., He, Q., & Yin, C. (2021). Is there an equality in the spatial distribution of urban vitality: A case study of Wuhan in China. *Open Geosciences, 13*(1), 469–481. https://doi.org/10.1515/geo-2020-0249
Pan, C., Zhou, J., & Huang, X. (2021). Impact of check-in data on urban vitality in the Macao Peninsula. *Scientific Programming, 2021*, 1–9. https://doi.org/10.1155/2021/7179965
Qiu, W., Li, W., Liu, X., & Huang, X. (2021). Subjectively measured streetscape perceptions to inform urban design strategies for Shanghai. *ISPRS International Journal of Geo-Information, 10*(8), 493. https://doi.org/10.3390/ijgi10080493
Qiu, W., Zhang, Z., Liu, X., Li, W., Li, X., Xu, X., & Huang, X. (2022). Subjective or objective measures of street environment, which are more effective in explaining housing prices? *Landscape and Urban Planning, 221*, Article 104358. https://doi.org/10.1016/j.landurbplan.2022.104358
Qiu, W., Li, W., Liu, X., Zhang, Z., Li, X., & Huang, X. (2023). Subjective and objective measures of streetscape perceptions: Relationships with property value in Shanghai. *Cities, 132*, Article 104037. https://doi.org/10.1016/j.cities.2022.104037
Row, A. T., & Jacobs, J. (1962). The death and life of great American cities. *Yale Law J, 71*, 1597. https://doi.org/10.2307/794509
Rui, J., & Othengrafen, F. (2023). Examining the role of innovative streets in enhancing urban mobility and livability for sustainable urban transition: A Review. *Sustainability, 15*(7), 5709. https://doi.org/10.3390/su15075709
Rui J., 2023a, Exploring the association between the settlement environment and residents' positive sentiments in urban villages and formal settlements in Shenzhen, Sustainable Cities and Society:104851. 10.1016/j.scs.2023.104851.
Rui, J. (2023b). Measuring streetscape perceptions from driveways and sidewalks to inform pedestrian-oriented street renewal in Düsseldorf. *Cities, 141*, Article 104472. https://doi.org/10.1016/j.cities.2023.104472
Ryan, R. M., Bernstein, J. H., & Brown, K. W. (2010). Weekends, work, and well-being: Psychological need satisfactions and day of the week effects on mood, vitality, and physical symptoms. *Journal of Social and Clinical Psychology, 29*(1), 95–122. https://doi.org/10.1521/jscp.2010.29.1.95
Sevtsuk, A., & Ratti, C. (2010). Learning from the aggregate data of mobile networks. *Journal of Urban technology, 17*(1), 41–60. https://doi.org/10.1080/10630731003597322
Shanahan, D. F., Franco, L., Lin, B. B., Gaston, K. J., & Fuller, R. A. (2016). The benefits of natural environments for physical activity. *Sports Medicine, 46*(7), 989–995. https://doi.org/10.1007/s40279-016-0502-4
Shannon, C. E. (1948). A Mathematical Theory of Communication. *The Bell System Technical Journal, 27*(3), 379–423. https://doi.org/10.1002/j.1538-7305.1948.tb01338.x
Shenzhen Municipal Planning and Land & Resources Commission (Marine Affairs Bureau). (2017). Shenzhen Urban Rail Transit Network Planning (2016-2035). Retrieved from https://csgx.szhome.com/uploadfiles/regulations/pdf/2018/12/121541151697161.PDF (Accessed July 2023).
Shenzhen Planning and Natural Resources Bureau. (2019). Shenzhen Urban Village Comprehensive Improvement Plan (2019-2025). Retrieved from http://www.sz.gov.cn/attachment/0/51/51731/1344686.pdf (Accessed June 2023).
Shenzhen Planning and Natural Resources Bureau. (2021). Shenzhen Urban Master Plan (2020-2035). Retrieved from http://www.sz.gov.cn/attachment/0/684/684608/1344759.pdf (Accessed June 2023).
Shi, Y., Zheng, J., & Pei, X. (2023). Measurement method and influencing mechanism of urban subdistrict vitality in shanghai based on multisource data. *Remote Sensing, 15*(4), 932.
Singh, R. (2016). Factors affecting walkability of neighborhoods. *Procedia - Social and Behavioral Sciences, 216*, 643–654. https://doi.org/10.1016/j.sbspro.2015.12.048
Smolders, K., De Kort, Y., & van den Berg, S. M. (2013). Daytime light exposure and feelings of vitality: Results of a field study during regular weekdays. *Journal of Environmental Psychology, 36*, 270–279. https://doi.org/10.1016/j.jenvp.2013.09.004
Sun, Y., & You, X. (2023). Do digital inclusive finance, innovation, and entrepreneurship activities stimulate vitality of the urban economy? Empirical evidence from the Yangtze River Delta, China. *Technology in Society, 72*, 102200. https://doi.org/10.1016/j.techsoc.2023.102200
Sung, H., & Lee, S. (2015). Residential built environment and walking activity: Empirical evidence of Jane Jacobs' urban vitality. *Transportation Research Part D Transport and Environment, 41*, 318–329. https://doi.org/10.1016/j.trd.2015.09.009
Tang, W., & Zhu, J. (2020). Informality and rural industry: Rethinking the impacts of E-Commerce on rural development in China. *Journal of Rural Studies, 75*, 20–29. https://doi.org/10.1016/j.jrurstud.2020.02.010
United Nations. (2017). Global indicator framework for the Sustainable Development Goals and targets of the 2030 Agenda for Sustainable Development. https://unstats.un.org/sdgs/indicators/Global Indicator Framework after 2021 refinement_Eng.pdf (Accessed June 2023).
Van Oostrum, M. (2022). Appropriating public space: transformations of public life and loose parts in urban villages. *Journal of Urbanism: International Research on Placemaking and Urban Sustainability, 15*(1), 84–105. https://doi.org/10.1080/17549175.2021.1886973
Wang, J. (2019). Inclusiveness and sharing, explicit and implicit mutual learning, livability predicted: Historical prospect and contemporary creation of urban vitality. *City Planning Review, 43*(12), 9–16.
Wen, M., Zheng, Z., & Niu, J. (2017). Psychological distress of rural-to-urban migrants in two Chinese cities: Shenzhen and Shanghai. *Asian Population Studies, 13*(1), 5–24. https://doi.org/10.1080/17441730.2016.1233655
Wu, J., Ta, N., Song, Y., Lin, J., & Chai, Y. (2018). Urban form breeds neighborhood vibrancy: A case study using a GPS-based activity survey in suburban Beijing. *Cities, 74*, 100–108. https://doi.org/10.1016/j.cities.2017.11.008
Wu, W., Ma, Z., Guo, J., Niu, X., & Zhao, K. (2022). Evaluating the effects of built environment on street vitality at the City level: an empirical research based on spatial panel Durbin model. *International Journal of Environmental Research and Public Health, 19*(3), 1664. https://doi.org/10.3390/ijerph19031664
Wu, C., Ye, Y., Gao, F., & Ye, X. (2023). Using street view images to examine the association between human perceptions of locale and urban vitality in Shenzhen, China. *Sustainable Cities and Society, 88*, Article 104291. https://doi.org/10.1016/j.scs.2022.104291
Xia, C., Yeh, A. G. O., & Zhang, A. (2020). Analyzing spatial relationships between urban land use intensity and urban vitality at street block level: A case study of five Chinese megacities. *Landscape Urban Planning, 193*, Article 103669. https://doi.org/10.1016/j.landurbplan.2019.103669
Yang, J., Cao, J., & Zhou, Y. (2021a). Elaborating non-linear associations and synergies of subway access and land uses with urban vitality in Shenzhen. *Transportation Research Part A: Policy and Practice, 144*, 74–88. https://doi.org/10.1016/j.tra.2020.11.014
Yang, Z., Chen, Y., Guo, G., Zheng, Z., & Wu, Z. (2021b). Using nighttime light data to identify the structure of polycentric cities and evaluate urban centers. *Science of The Total Environment, 780*, Article 146586. https://doi.org/10.1016/j.scitotenv.2021.146586
Ye, Y., Li, D., & Liu, X. (2018). How block density and typology affect urban vitality: An exploratory analysis in Shenzhen, China. *Urban Geography, 39*(4), 631–652. https://doi.org/10.1080/02723638.2017.1381536
Yin, L., & Wang, Z. (2016). Measuring visual enclosure for street walkability: Using machine learning algorithms and google street view imagery. *Applied Geography, 76*, 147–153. https://doi.org/10.1016/j.apgeog.2016.09.024
Yin, L., & Zhang, H. (2021). Building walkable and safe neighborhoods: Assessing the built environment characteristics for pedestrian safety in Buffalo, NY. *Journal of Transport & Health, 22*, Article 101129. https://doi.org/10.1016/j.jth.2021.101129
Yuan, L., Hou, Q., Jiang, Z., Feng, J., & Yan, S. (2022). Volo: Vision outlooker for visual recognition. *IEEE Transactions on Pattern Analysis and Machine Intelligence*. https://doi.org/10.1109/TPAMI.2022.3206108
Yue, W., Chen, Y., Zhang, Q., & Liu, Y. (2019). Spatial explicit assessment of urban vitality using multi-source data: A case of Shanghai, China. *Sustainability, 11*(3), 638. https://doi.org/10.3390/su11030638

Zhang A., Li W., Wu J., Lin J., Chu J., Xia C., 2021a, How can the urban landscape affect urban vitality at the street block level? A case study of 15 metropolises in China, Environment and Planning B: Urban Analytics and City Science 48(5):1245-1262. 10.1177/2399808320924425.

Zhang, J., Liu, X., Tan, X., Jia, T., Senousi, A. M., Huang, J., Yin, L., & Zhang, F. (2021b). Nighttime vitality and its relationship to urban diversity: an exploratory analysis in Shenzhen, China. *IEEE Journal of Selected Topics in Applied Earth Observations and Remote Sensing, 15*, 309–322. https://doi.org/10.1109/JSTARS.2021.3130763

Zhang, Y., Li, S., Dong, R., Deng, H., Fu, X., Wang, C., Yu, T., Jia, T., & Zhao, J. (2021c). Quantifying physical and psychological perceptions of urban scenes using deep learning. *Land Use Policy, 111*, Article 105762. https://doi.org/10.1016/j.landusepol.2021.105762

Zhang, Z., Long, Y., Chen, L., & Chen, C. (2021d). Assessing personal exposure to urban greenery using wearable cameras and machine learning. *Cities, 109*, Article 103006. https://doi.org/10.1016/j.cities.2020.103006

Zhang, W., Lu, D., Zhao, Y., Luo, X., & Yin, J. (2022). Incorporating polycentric development and neighborhood life-circle planning for reducing driving in Beijing: Nonlinear and threshold analysis. *Cities, 121*, Article 103488. https://doi.org/10.1016/j.cities.2021.103488

Zhou, Q., & Luo, J. (2017). The study on evaluation method of urban network security in the big data era. *Intelligent Automation and Soft Computing, 1-6*. https://doi.org/10.1080/10798587.2016.1267444